AD-A142 402 ENERGY RELEASE AND FLUID DYNAMICS IN MULTIPHASE SYSTEMS 1/2
(U) SCIENCE APPLICATIONS INC MCLEAN VA K KAILASANATH
18 APR 84 SAI-84/1093 N00014-82-C-2037

UNCLASSIFIED F/G 20/4 NL

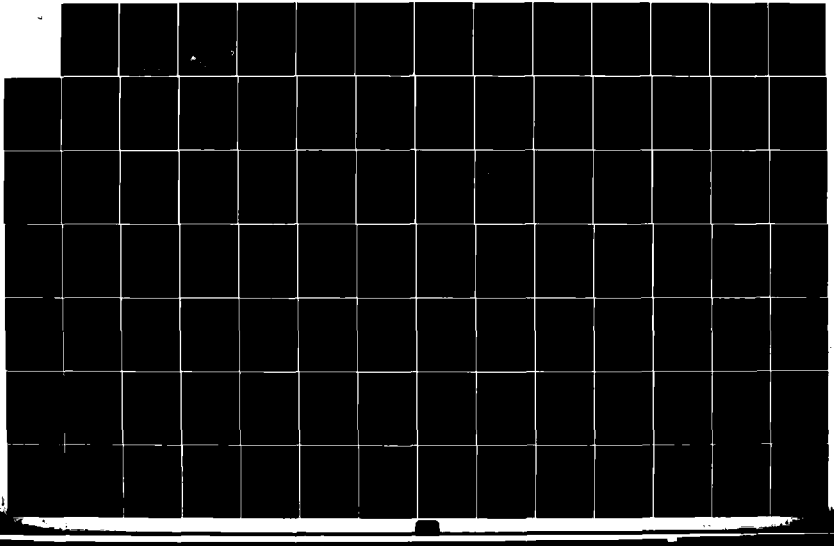

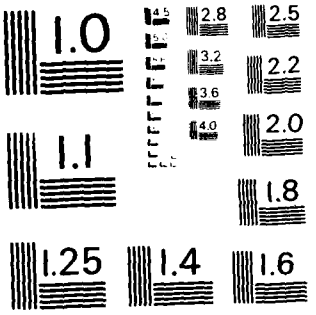

(12)

AD-A142 402

ENERGY RELEASE AND FLUID DYNAMICS IN MULTIPHASE SYSTEMS

K. KAILASANATH

FINAL REPORT NO. SAI 84/1093

SCIENCE APPLICATIONS, INC.

ENERGY RELEASE AND FLUID DYNAMICS IN MULTIPHASE SYSTEMS

K. KAILASANATH

FINAL REPORT NO. SAI 84/1093

SCIENCE APPLICATIONS, INC.

Post Office Box 1303, 1710 Goodridge Drive, McLean, Virginia 22102, (703) 821-4300

ENERGY RELEASE AND FLUID DYNAMICS

IN MULTIPHASE SYSTEMS

K. Kailasanath

FINAL REPORT NO. SAI 84/1093

Submitted to

Laboratory for Computational Physics
4555 Overlook Avenue, S.W.
Naval Research Laboratory
Washington, D.C. 20375

Prepared under:

Contract No. N00014-82-C-2037

by

Science Applications, Inc.
1710 Goodridge Drive
McLean, Virginia 22102

April 18, 1984

SCIENCE APPLICATIONS, INCORPORATED

1710 Goodridge Drive, McLean, Virginia 22102 (703) 734-5840

TABLE OF CONTENTS

GENERAL DISCUSSION

In the following discussion we will summarize the work performed by Science Applications, Inc. (SAI) on "Energy Release and Fluid Dynamics in Multiphase Systems" (additional effort under Contract #N00014-82-C-2037, SAI Project #1-157-18-519-00) during the technical performance period ending February 1984. During this contract period, our attention was focussed primarily on: (1) studying the structure and propagation of multidimensional detonations, and (2) shock initiation of detonations with an emphasis on power-energy relations. The efforts and accomplishments in each of these areas is described below in some detail.

Structure and Propagation of Multidimensional Detonations

The propagation of self-sustained detonations is a complex, multidimensional process involving interactions between incident shocks, Mach stems, transverse waves and boundaries of the regions through which the detonation is moving[1,2,3]. Experiments have shown that a propagating detonation leaves a very regular, cell-like pattern on the sidewalls of the confining chamber[1,4,5]. These patterns are etched by the triple-point formed at the front of the detonation by the intersection of the transverse wave with the incident shock and the Mach stem. Thus, the cell patterns are histories of the location of the triple point. The size and regularity of this cell structure is

characteristic of the particular combination of initial material conditions, such as composition, density and pressure and the geometry of the confining chamber[1,6,7]. An understanding of the cell structure is vital for quantifying the detonability of gaseous mixtures.

We have performed a computational study of self-sustained detonations with emphasis on finding a systematic computational method to estimate the natural cell size for a particular material. In addition, by examining the behavior of the transverse wave structure, we have been able to develop insight into the mechanism of propagation of self-sustained detonations.

We have concentrated on planar mode detonations, which are two-dimensional and unsteady in the neighborhood of their detonation fronts. The numerical model used to perform the simulations solves the time-dependent conservation equations for mass, momentum and energy [8] in two dimensions using one variant of the Flux-Corrected Transport (FCT) algorithm[9]. In addition to the solution of the convection terms by FCT we have included an induction parameter model which is a phenomenology developed to reproduce the correct ignition delays and subsequent energy release due to chemical reactions[10].

Recent schlieren photographs of detonations in low pressure hydrogen-oxygen-argon mixtures and numerical simulations of propagating detonations showed the presence

of unreacted pockets of gas behind the shock front-Mach stem structure[11]. These pockets are surrounded by completely burned gas, and they in turn burn more slowly due to their low temperatures. So we first used the numerical simulations to study the idealized problem of a slowly burning pocket of material behind a two-dimensional planar detonation (one without any initial transverse structure). This study showed that the burning of a large enough pocket provides a sufficient perturbation to the planar detonation to cause it to form a multidimensional structure. This is an equilibrium configuration since it repeats exactly at equally spaced intervals as the detonation propagates down the channel. It is also an unique structure since changing the size and orientation of the initial perturbation does not affect the final state. We then developed a computational method of determining the cell size from such simulations. The method involves simulating systems with channel widths both larger and smaller than the transverse cell spacing. This approach, tested on a mixture of hydrogen, oxygen and argon, provides us with an estimate of the cell size which is in excellent agreement with experimental data. This accomplishment is very significant since direct experimental measurement of detonation cell size is often not practical or feasible and is always very difficult and expensive.

The numerical simulations have not only provided us with a method of determining the cell size from first principles but have also provided insight into some aspects of the mechanism by which a self-sustained detonation propagates. The evolution of the curvature of the transverse wave appears to be a crucial feature. First we observed in the simulations that the final result of a transverse wave collision is a reversal of the curvature of the transverse wave. This implies that the natural cell size might be defined as that distance between two triple points which occurs when the curvature of two oppositely moving transverse waves goes nearly to zero. This is substantiated by the evidence obtained in the simulations that if the tails of the transverse waves collide first, flattening of the cell occurs. Further, if the heads of the transverse waves collide first, an unburned pocket can form. Thus, the simulations have also allowed us to put into perspective the previous calculations on the formation of unburned gas pockets behind detonation fronts[11].

A portion of this work was presented at the 36th Meeting of the American Physical Society, Division of Fluid Dynamics (November 1983) with the title "Numerical Simulations of the Effects of Unburned Gas Pockets behind Propagating Detonations". Portions of the work will be presented at the Twentieth International Symposium on

Combustion (August 1984), an abstract of which is included in this report as Appendix A entitled "Determination of Detonation Cell Size Using Multi-dimensional Numerical Simulations". A more complete version of this study has been submitted to the journal, Combustion and Flame, and is included has as Appendix B entitled, "Numerical Simulations of the Structure and Propagation of Self-Sustained Detonations".

Shock Initiation of Detonations

A simple theoretical model was developed to determine the relation between the power and energy required for the shock initiation of gaseous detonations. Some details of the model and its initial application to the study of detonations in oxy-acetylene mixtures have already been presented in a previous report[12]. During this contract year, further work on refining the model and applying it to study the shock initiation of detonations in a hydrogen-air mixture was carried out.

It was reported earlier that the model successfully explained the qualitative differences in the power-energy relations obtained from two different experimental arrangements[12,13]. The model also gave qualitatively good predictions of the power-energy relation for the initiation of cylindrical detonations in an acetylene-oxygen-nitrogen mixture[13]. However, the minimum power and the minimum energy predicted by the model were quantita-

tively different from those obtained experimentally. One reason for the difference is the uncertainity in the appropriate time to be used for the critical time for which energy must be deposited in order to initiate a detonation[14]. During this contract year, we have addressed this issue in some detail by comparing the results from the theoretical model to those obtained from detailed numerical simulations on the initiation of planar detonations in a hydrogen-air mixture.

The one-dimensional reactive shock model[15] used to perform the detailed simulations solves the time-dependent conservation equations for mass, momentum and energy coupled to the equations describing the chemical kinetics. The model uses an explicit, Eulerian finite difference formulation with a sliding rezone capability to provide resolution around moving gradients. The solutions of the equations describing the fluid dynamics and the chemistry of the problem are coupled using time-step splitting techniques[8].

We first used the theoretical model to determine the power-energy relations for the initiation of planar detonations in a hydrogen-air mixture. The time duration necessary for the successful initiation was assumed to be equal to the chemical induction time of the mixture. The induction time used was obtained by integrating the same chemical kinetics rate equations used in the detailed

simulations. We then set up the numerical model to simulate the same problem solved by the theoretical model.

The results from the detailed simulations agreed with the predictions of the theoretical model when the Mach number of the shock wave was high. However for low Mach numbers, the detailed simulations showed initiation with lower energies than those predicted by the theoretical model. A closer look at the results showed that the pressures and temperatures in the shocked material were in the weak-ignition regime and therefore very sensitive to perturbations[16].

In order to evaluate quantitatively how a specific type of perturbation affects ignition, we then simulated the effects of sound waves in a hydrogen-air mixture by reconfiguring the numerical model described above. This gave us a quantitative relation between the induction time and the sound waves of various amplitudes and frequencies. The effect of such sound wave perturbations on the power-energy relation has also been determined.

In addition to the above, further studies on the initiation of detonations in an acetylene-oxygen-nitrogen mixture was also carried out. Here the primary focus was on evaluating the importance of using a variable γ, the ratio of specific heats. For this purpose the power-energy relations were determined using various constant γ's and also using a variable γ. This study

showed that using constant γ's not only changes the values of the minimum power and minimum energy but also the Mach number corresponding to these minimum values.

A portion of the work described above was presented at the Ninth International Colloquim on the Dynamics of Explosions and Reactive Systems (July 1983) and has been accepted for publication in a forthcoming volume of the series, "Progress in Astronautics and Aeronautics". This part of the work is included in this report as Appendix C entitled, "Power-Energy Relations for the Direct Initiation of Gaseous Detonations". Portions of the work have also been presented at the 1983 Fall Meeting of The Combustion Institute (November 1983), a short version of which is included here as Appendix D with the title, "Shock Initiation of Detonations in Hydrogen-Air Mixtures". A more detailed account of part of the work described above has also been published as NRL Memorandum Report #5179, "The Relation Between Power and Energy in the Shock Initiation of Detonations - I". This memo report is included here as Appendix E. Part II of this memo report is currently in preparation.

REFERENCES

1. Strehlow, R.A.: Fundamentals of Combustion, Chapter 9, Krieger Pub. Co., 1979.
2. Ficket, W. and Davis, W.C.: Detonation, Chapter 7, University of California Press, 1979.
3. Lee, J.H.S.: Ann. Rev. Phys. Chem. 28, 75 (1977).
4. Oppenheim, A.K.: Astro. Acta 11, 391 (1965).
5. Lee, J.H., Soloukhin, R.I. and Oppenheim, A.K.: Astro. Acta 14, 565 (1969).
6. Strehlow, R.A., Liaugminas, R., Watson, R.H. and Eyman, J.R.: Eleventh Symposium (International) on Combustion, p. 683, The Combustion Institute, 1967.
7. Strehlow, R.A.: Astro. Acta 14, 539 (1969).
8. Oran, E.S. and Boris, J.P.: Prog. Ener. Comb. Sci. 7, 1 (1981).
9. Boris, J.P. and Book, D.L.: Methods in Computational Physics, Vol. 16, p. 85, Academic Press, 1976. Also, Boris, J.P.: Flux-Corrected Transport Modules for Solving Generalized Continuity Equations, Naval Research Laboratory Memorandum Report 3237, 1976.
10. Oran, E.S., Boris, J.P., Young, T., Flanigan, M., Burks, T., and Picone, M.: Eighteenth Symposium (International) on Combustion, p. 1641, The Combustion Institute, 1981.
11. Oran, E.S., Young, T.R., Boris, J.P., Picone, J.M. and Edwards, D.H.: Nineteenth Symposium

(International) on Combustion, p. 573, The Combustion Institute, 1982.

12. Kailasanath, K. and Hyman, E.: Energy Release and Fluid Dynamics in Multiphase Systems, SAI 84-122-WA, 1983.

13. Kailasanath, K. and Oran, E.S.: Power-Energy Relations for the Direct Initiation of Detonations in Oxy-Acetylene Mixtures", Paper No. WSCI-83-35. Presented at the Spring Meeting of the Western States Section of the Combustion Institute, 1983.

14. Kailasanath, K. and Oran, E.S., The Relation between Power and Energy in the Shock Initiation of Detonations-I. Basic Theoretical Considerations and the Effect of Geometry. NRL Memorandum Report No. 5179, Naval Research Laboratory, Washington, DC, 1983.

15. Oran, E.S., Young, T.R., and Boris, J.P., Seventeenth Symposium (international) on Combustion, The Combustion Institute, Pittsburgh, PA, p. 43 (1979).

16. Oran, E.S. and Boris, J.P., Combust. Flame 48, 149 (1982).

APPENDIX A

DETERMINATION OF DETONATION CELL SIZE USING MULTI-DIMENSIONAL NUMERICAL SIMULATIONS

DETERMINATION OF DETONATION CELL SIZE USING MULTI-DIMENSIONAL NUMERICAL SIMULATIONS

K.Kailasanath *, E.S. Oran, J.P. Boris and T.R. Young

Laboratory for Computational Physics
Naval Research Laboratory
Washington, D.C. 20375

The propagation of self-sustained gaseous detonations is a complex, multidimensional process involving interactions between incident shocks, Mach stems, transverse waves and boundaries of the regions through which the detonation is moving. Experiments have shown that a propagating detonation leaves a very regular, cell-like pattern on the sidewalls of the confining chamber. These patterns are etched by the triple-point formed at the front of the detonation by the intersection of the transverse wave with the incident shock and the Mach stem. Thus the cell patterns are histories of the location of the triple point. The size and regularity of this cell structure is characteristic of the particular combination of initial material conditions, such as composition, density and pressure and the geometry of the confining chamber. An understanding of the cell structure is vital for quantifying the detonability of gaseous mixtures. Direct experimental measurement of detonation cell size is often not practical or feasible and is always very difficult . Therefore we have developed a computational method of determining the natural cell size of a self-sustained detonation.

We have concentrated on planar mode detonations, which are two-dimensional and unsteady in the neighborhood of their detonation fronts. We have used the numerical simulations to develope a computational method of determining the natural cell size of a self-sustained detonation. The systematic approach involves simulating systems with tube heights both larger and smaller than the transverse cell spacing. This approach, tested on a mixture of hydrogen, oxygen and argon, provides us with an estimate of the cell size which is in excellent agreement with experimental data.

The numerical simulations have not only provided us with a method of determining the cell size from first principles but have also provided insight into some aspects of the mechanism by which a self-sustained detonation propagates. The evolution of the curvature of the transverse wave appears to be a crucial feature. Depending on the curvature of the transverse wave at the time of its reflection from either a neighboring transverse wave or a wall, the cell is either flattened or pockets of unreacted gas can be formed.

We will describe some numerical simulations and graphically show details of the detonation structure. Comparisons to experimental data will also be presented which show that these numerical simulations have been able to predict the detonation cell sizes accurately.

---

* Science Applications, Inc., Mclean, VA.

APPENDIX B

NUMERICAL SIMULATIONS OF THE STRUCTURE AND PROPAGATION OF SELF-SUSTAINED DETONATIONS

NUMERICAL SIMULATIONS OF THE STRUCTURE AND PROPAGATION OF SELF-SUSTAINED DETONATIONS

K. Kailasanath*, E.S. Oran, J.P. Boris and T.R. Young

Laboratory for Computational Physics
Naval Research Laboratory
Washington, D.C. 20375

* Science Applications, Inc., McLean, Va.

Subject Headings:

(35) Detonation
(23) Theory of Deflagration and Detonation
(22) Supersonic Flow with Reaction

Address Correspondence to:

Dr. E.S. Oran
Code 4040
Naval Research Laboratory
Washington, D.C. 20375

ABSTRACT

Two-dimensional time-dependent numerical simulations have been performed to determine a computational method of determining the natural cell size of a self-sustained detonation. The systematic approach developed involves simulating systems with tube heights both larger and smaller than the transverse cell spacing. This approach, tested on a mixture of hydrogen, oxygen and argon, provided us with an estimate of the cell size.

The simulations also provided insight into some aspects of the mechanism by which a self-sustained detonation propagates. The evolution of the curvature of the transverse wave appears to be the crucial feature. Depending on the curvature of the transverse wave at the time of its reflection from either a neighboring transverse wave or a wall, the cell is either flattened or pockets of unreacted gas can be formed.

I. INTRODUCTION

The propagation of self-sustained gaseous detonations is a complex, multi-dimensional process involving interactions between incident shocks, Mach stems, transverse waves and boundaries of the regions through which the detonation is moving[1,2,3]. The triple points formed at the intersection of the transverse wave with the Mach stem and the incident shock trace out the patterns we call detonation cells[1,4,5]. Extensive experimental data[6,7,8] has shown that the size and regularity of this cell structure is characteristic of the particular combination of initial material conditions, such as composition, density and pressure[1,9,10]. Theoretical efforts[6,11,12,16] to explain the cell size vary in accuracy and in some cases predict sizes within a factor of two[2]. Numerical simulations have shown that these cells can be formed by perturbing a planar one-dimensional detonation, but they also show some dependence on initial conditions[13]. Here we present a computational study of self-sustained detonations with emphasis on finding a systematic computational method to estimate the natural cell size for a particular material. In addition, by examining the behavior of the transverse wave structure, we have been able to develop insight into the mechanism of propagation of self-sustained detonations.

We have concentrated on planar mode detonations, which are two-dimensional and unsteady in the neighborhood of their detonation fronts. They are obtained experimentally in tubes of narrow, rectangular cross section when the preferred transverse wave spacing of the detonation is at least five times the width of the tube[1,6]. This study extends the ideas and methods described at the 19th Combustion Symposium[14] in which a time-dependent two-dimensional numerical model[15] was used to study the formation of unreacted gas pockets within the detonation cell of a marginal detonation. In the simulations discussed in this paper, we perturb a planar propagating detonation, i.e., one without any initial transverse structure, with a large pocket of unburned material behind the detonation front.

First we show that the burning of a large enough pocket provides a sufficient perturbation to the planar detonation to cause it to form a multi-dimensional structure. This is an equilibrium configuration[16] since it repeats exactly at equally spaced intervals as the detonation propagates down the channel. It is also an unique structure since changing the size and orientation of the initial perturbation does not affect the final state. We then describe a procedure for determining the detonation cell size from such numerical simulations based on systematically increasing the tube height in the computation. In this way a relatively limited set of calculations can give an estimate of the cell size from a first principles calculation. This approach has provided us not only with an *estimate of* the detonation cell size, but also with a picture of the role played by the transverse wave in a self-sustained detonation. Finally, the set of calculations described below has allowed us to put into perspective the previous calculations of the formation of unburned gas pockets behind detonation fronts.

II. THE NUMERICAL MODEL

The numerical model used to perform the simulations described in this paper solves the time-dependent conservation equations for mass, momentum and energy[17] in two dimensions using one variant of the Flux-Corrected Transport (FCT) algorithm[18]. This model with various initial and boundary conditions has been used to study single and double Mach reflections[19], mixing and vortex formation at material interfaces[20] and the formation of unreacted gas pockets behind propagating detonations[14,19]. Thus its ability to calculate complicated shock structures has been tested extensively against theory, experiment and independent computations.

In addition to the solution of the convection terms by FCT, we have included an induction parameter model which is a phenomenology developed to reproduce the correct ignition delays and subsequent energy release due to chemical reactions[15]. In this model three quantities must be specified: the time before any energy is

released (the chemical induction time), the time it takes to release the energy, and the total amount of energy released. An induction parameter[15,21] is then defined which is a measure of how long the material has remained at a given temperature and pressure. In the calculations this quantity is convected with the fluid and is used to indicate when the available chemical energy should be released. For the supersonic reacting flows we are studying here, diffusive effects such as thermal conduction, viscosity and molecular diffusion are small. Thus we need to consider only the strong interaction between gas dynamics and chemistry. The convection and energy release algorithms are coupled by previously described methods[17].

In order to economically resolve the details of the flowfield behind the moving reactive shock front, an adaptive gridding method is used. A region of fine zones in the x-direction surrounds and moves with the shock front[15,17]. The remaining cells in the x-direction are evenly spaced, except that a smooth transition from fine to coarse zones is enforced. The cells in the y-direction are evenly spaced and have the same size as the fine zones in the x-direction. In the calculations described below, a 150 x 50 mesh was used which meant fine zones in the range 0.1 - 0.18 cm and coarse zones in the range 1.0 - 1.8 cm for the different systems simulated. Computational timesteps were in the range 0.1 - 0.18 microseconds. The calculations generally required 2000-3000 timesteps to reach an equilibrium detonation configuration. One calculation typically requires 90 minutes of CPU time on the Texas Instruments ASC computer.

III. RESULTS AND DISCUSSION

All the simulations described below were initialized by placing an elliptical pocket of unburnt gas behind a planar detonation propagating into a 65 torr (8.66 kPa), 298 K stoichiometric hydrogen-oxygen mixture diluted with 60% argon. Thus in these simulations the pockets are used as a device for initiating the perturbation. Tubes of 5, 7 and 9 cm height were simulated.

Determination of Detonation Cell Size

The first calculation simulated a tube 5 cm high, which we estimated from the experimental data to be close to the natural detonation cell size of the mixture[7]. An unburnt gas pocket, placed symmetrically behind the planar detonation, generates pressure waves as it burns. These waves interact with the incident shock front causing the front to curve outwards and after a short time a portion of the incident shock reflects from the side walls of the tube. The transverse waves formed are strengthed due to collisions with each other and the walls, eventually forming the pair of well defined triple points seen in Fig. 1. This figure is a composite of seven snapshots of the density contours at intervals of 10 microseconds. In the first frame the transverse waves are moving away from each other and towards the wall, by the fourth frame they have reflected from the walls and are moving towards the center of the tube, and by frame 7 they are again moving towards the wall after colliding with each other. Small deviations in the contours in Fig. 1 at the symmetrical locations above and below the centerline are a result of small asymmetries in the calculation.

Figure 1 shows that the triple point structure does not immediately bounce off when it hits the wall, indicating that a complete detonation cell has not been formed. The pattern of the triple points for this calculation is clearer in Fig. 2A, which shows a time and space gap at the walls as the structure reforms. Increasing the height of the tube to 7 cm, as shown in Fig. 2B, results in a considerably reduced gap in the path of the triple points propagating from the walls. Finally, the locus of the triple points for a 9 cm tube, shown in Fig. 2C, forms a complete detonation cell and what appears to be partial structures above and below it. From the figure we estimate the cell height and length to be about 8.5 cm and 19.6 cm, respectively.

The surprising feature of the calculations shown in Figs. 2 is the flattened shape of the cell when the tube height is less than the cell height (e.g., Fig. 2A).

Below we provide an explanation of this behavior based on observations of the temperature, pressure and density contours around the transverse wave structure. We also provide evidence that the varying cell shapes shown in Figs. 2A are a result of the shape and curvaturve of the transverse wave as it collides with the wall.

Propagation of Self-Sustained Detonations

Figure 3 shows temperature contours from the 5 cm tube simulation at six different times at intervals of 10 microseconds. At cycle 2400 the transverse waves have already collided with each other and are moving towards the wall at an angle indicated by the arrows. It is useful to focus on the shaded region between the 1300 K and 2100 K contours since as it evolves it reflects the changing size of the induction zone. First we note the well-known fact that behind the transverse wave this region is very narrow and the 2100 K contour is close to the Mach stem. This is because the higher temperatures and pressures caused by the passage of the transverse wave decrease the size of the induction zone. Ahead of the transverse wave the region is much more extended behind the incident shock. Energy release behind a transverse wave generates pressure waves which drive it towards the wall. Thus the transverse waves are driven into the shocked but as yet unburned gas mixture ahead of it. This energy release also drives the Mach stem outward causing the characteristic bulge seen in the figures. This expansion causes a decrease in the velocity of the Mach stem and by cycle 2500 the reaction zone has begun to decouple from the Mach stem behind the transverse wave. By cycle 2600, the reaction zone is even more separated from the shock front. In the absence of walls, this separation would continue to grow until either the reaction zone and shock front became so decoupled that the detonation dies, or until ignition occurrs spontaneously due to heating for a long enough time in the induction region. This latter effect appears to occur in the 9 cm simulation described above in which triple points appear spontaneously in the

induction zones just before reflection of the transverse waves from the walls. However, the detonation cell in this 5 cm case is re-initiated by the collision between the transverse waves and the walls. The collision reverses the direction of motion of the transverse waves and so the transverse waves again encounter shocked but unburned mixtures ahead of them. The transverse waves move towards each other and by cycle 2900 they have collided in the center of the tube. Again we observe a large induction zone beginning to form before the collision so that when the transverse waves reverse direction they again encounter unburned material to propagate into.

This picture corroborates the rough criterion given by Fickett and Davis[2], who maintained that in a detonation cell, a large enough induction zone must form between two transverse waves receeding from each other. Then when the waves collide and their directions are reversed, they encounter enough unreacted material to sustain their propagation through to the next collision. Although this concept is supported by the calculations shown above, it does not give us a criterion for determining a cell size: we saw above that the 5 cm case is smaller than a detonation cell size, and yet we obtain a self-propagating repeatable structure.

To better understand the factors that determine the size of a cell, we must examine the curvature of the transverse wave as it reflects from the wall or another transverse wave. Consider the pressure contours for the 5 cm case shown in Fig. 4., in which the location of the transverse wave, incident shock and Mach stems are marked. For purposes of this explanation we call the 'head' of the transverse wave that portion at and close to the triple point, and we call the 'tail' that region of the transverse wave extending back towards the burned material. At cycle 3200 the transverse waves are moving towards each other, and we observe that the distance between the two heads is larger than the distance between the two tails. The pressure contours around the transverse wave outline

its curvature. The same curvature is evident at cycle ~300, from which we conclude that the tails of the transverse waves are going to collide with each other earlier than the heads. Cycle 3600 is a time after the collision of the transverse waves at the center of the tube and the cell has been reinitiated. Comparing the figures here, we conclude that the curvature of the transverse wave is reversed at or around the time of collision. Also at cycle 3600, the heads of the transverse wave are closer to each other than the tails. Therefore the tails of the transverse wave collide with and reflect from the walls earlier than the heads. From this we see that such reflection causes a higher pressure difference across the tail segment of the transverse wave as compared to that across the unreflected front segment. This high pressure region pushes the incident shock front forward and results in the flattened detonation cell we saw in Figs. 1 and 2A.

The above observations are for the 5 cm tube for which the natural detonation cell height is larger than 5 cm. Now consider the 7 cm case. Here the transverse wave can travel further, become weaker before collisions, and the inclination of the transverse waves to the tube walls is less. This is evident upon inspection of figures similar to Fig. 4 for the 7 cm case. If the height of the tube is exactly equal to the cell height, we expect the transverse wave to be parallel to the wall at the time of reflection and then every segment of it reflects from the wall at about the same time. The locus of the triple points in the 7 cm tube shown in Fig. 2B corroborates this argument since the gap in the path of the triple points almost disappears with the increase in the tube height. Furthermore, from the discussion above of the mechanism sustaining detonation propagation, we see that if the tube height is significantly larger than the detonation cell height, we expect generation of new triple points due to local instabilities occurring in the shocked material ahead of the transverse waves. This produces a new pair of transverse waves propagating towards the two transverse waves already present in the system. The new and old waves then collide

with each other when the transverse wave spacing equals the detonation cell height. Therefore in a tube slightly larger than the detonation cell height we would observe four transverse waves at certain periods in the detonation cell cycle as well as a complete detonation cell within the tube. This is what is seen in Fig. 2C for the 9 cm simulation.

Formation of Unburned Gas Pockets

In the 9 cm tube case shown in Fig. 2C we also observed the presence of unburned gas pockets near the walls behind the detonation front[14,19]. The origin of these pockets in the calculation can be explained by extending the argument put forth above on the inclination of the transverse wave. Consider a case for which the tube height is slightly larger than the detonation cell height. In this case, a transverse wave moving towards the walls, which does not encounter another transverse wave moving in the opposite direction, continues to propagate though considerably weakened. However, here the head of the transverse wave reflects earlier than the rear segment. As previously discussed[14], this results in a portion of the gas near the head of the transverse wave burning first and effectively cutting off a gas pocket. For an unburned gas pocket to form in this way, ignition near the walls must be delayed by some effect. Thus an unburned pocket is more likely to occur in marginally detonable mixtures such as the one considered here or at the walls in real systems where there are heat losses.

Simulations with Asymmetric Initiation

A number of simulations were performed in which the initiating perturbing pocket was placed asymmetrically so that its axis was at an angle to the planar detonation front. In these cases unsymmetrical triple points evolved and disappeared, quickly creating a very irregular cell structures. However, the system eventually evolved into the symmetrical cases and produced the cell structure shown in Figs. 2.

In another case we tried to take advantage of the symmetry about the centerline apparent in Figs. 2. In an earlier paper[14] we speculated that simulating a detonation in a tube which is half the cell height would force a half cell structure and be equivalent to half of a simulation of a full cell. To test this, we compared two calculations: a 10 cm tube in which a symmetrical pocket was used (similar to those in Fig. 2), and a 5 cm tube in which the upper half of a symmetrical pocket was placed on the lower wall. The 10 cm calculation indeed verified the observations in the 9 cm case: a cell of about 8.5 cm was formed in the center of the system and there was not room enough for another full cell to appear in the calculation. The 5 cm case initially looked like the upper half of the 10 cm case, but as time went on it became irregular and eventually evolved into the regular structure shown in the 5 cm calculation in Fig. 2A. These results confirm that the equilibrium structures obtained in the numerical simulations are independent of the initial pertubations. From this we conclude that simulating half-cells can be misleading. Here we found in the 5 cm asymmetric simulation (which was the upper half of the 10 cm case) that two structures are vying with each other for dominance: one such as in Fig. 2A and another which is half of the 10 cm calculation. The dominant mode of propagation eventually wipes out the subdominant mode. These results are consistent with the ideas described above concerning the structure of the transverse wave at the time of reflection.

IV. SUMMARY AND CONCLUSIONS

The simulations described above present a systematic approach for numerically determining detonation cell sizes. The basic ingredients in such simulations are a model for the chemical kinetics and a convective transport algorithm that is accurate enough to resolve shocks, Mach structures, and reaction zones. The convective transport algorithm used here has been tested extensively and we understand its capabilities and limitations. The induction parameter model used for the chemical kinetics is a phenomenological model derived from a detailed

chemical reaction rate mechanism. Such a parametric model has the potential of being useful in calculations such as these when either we cannot afford to use the full chemical reaction scheme or when such a scheme is not available but we have experimental data on ignition and energy release times. However, the only way to benchmark the coupled models is by comparing to experiments and to calculations containing the detailed chemical rate scheme. With increased computational speed and memory available, we are close to being able to include a detailed chemical reaction model at least for hydrogen-oxygen combustion.

We also have found that the simulations are useful for graphically displaying the detailed, evolving structure of the detonation front. The results shown above have provided insight into some aspects of the mechanism by which a self-sustaining detonation propagates. They have indicated that the curvature of the transverse wave at the time of its reflection is extremely important to the resulting cell structure. First we observe in the simulations that the final result of a transverse wave collision is a reversal of the curvature of the transverse wave. This implies that the natural cell size might be defined as that distance between two triple points which occurs when the curvature of two oppositely moving transverse waves goes nearly to zero. This is substantiated by the evidence given above that if the tails of a transverse wave collide first, flattening of the cell occurs. Further, if the heads of the transverse waves collide first, an unburned pocket can form.

Future calculations will test several aspects of the results presented above. First, the approach for predicting cell sizes must now be tested for a wide range of hydrogen-oxygen mixtures, especially those whose detonation cell sizes are well-known from experiments. This should provide a better test of the validity of the induction parameter model for the chemistry, and tell us when and if we need more complete chemical models. Then calculations such as these with an induction parameter model can be applied to methane and other

materials for which good chemical kinetic data exists. Finally, more resolved calculations must be done and the details of the structure and evolution of the transverse wave must be compared to previous observations[9, 22-26]. The observations presented of the structure are very convincing, but much more intermediate data is required for clarity and verification.

ACKNOWLEDGEMENTS

The authors are indebted to Dr. J.M. Picone for his invaluable help with the code, and especially with the graphics. We would like to acknowledge helpful conversations with Professors D.H. Edwards, J.H. Lee, T. Fujiwara, R. Strehlow and A.K. Oppenheim. This work was sponsored by the Office of Naval Research through the Naval Research Laboratory.

REFERENCES

1. Strehlow, R.A.: Comb. Flame 12, 81 (1968). Also, Strehlow, R.A..: Fundamentals of Combustion, Chapt. 9, Krieger Pub. Co., 1979.
2. Fickett, W. and Davis, W.C.: Detonation, Chapt. 7, University of California Press, 1979.
3. Lee, J.H.S.: Ann. Rev. Phys. Chem. 28, 75 (1977).
4. Oppenheim, A.K.: Astro. Acta 11, 391 (1965).
5. Lee, J.H., Soloukhin, R.I and Oppenheim, A.K.: Astro. Acta 14, 565, (1969).
6. Strehlow, R.A., Maurer, R.E. and Rajan, S.: AIAA J. 7, 323, (1969).
7. Strehlow, R.A. and Engel, C.D.: AIAA J. 7, 492, (1969).
8. Knystautas, R., Lee, J.H. and Guirao, C.M.: Comb. Flame 48, 63 (1982).
9. Strehlow, R.A., Liaugminas, R., Watson, R.H., and Eyman, J.R.: Eleventh Symposium (International) on Combustion, p. 683, The Combustion Institute, 1967.
10. Strehlow, R.A.: Astro. Acta 14, 539 (1969).
11. Barthel, H.O. and Strehlow, R.A.: Phys. Fluids 9, 1896 (1966).
12. Barthel, H.O.: Phys. Fluids 17, 1547 (1974).
13. Taki, S. and Fujiwara, T.: AIAA J. 16, 73 (1978). Also, Eighteenth Symposium (International) on Combustion, p. 1671, The Combustion Institute, 1981.
14. Oran, E.S., Young, T.R., Boris, J.P., Picone J.M. and Edwards, D.H.: Nineteenth Symposium (International) on Combustion, p. 573, The Combustion Institute, 1982.
15. Oran, E.S., Boris, J.P., Young, T., Flanigan, M., Burks, T., and Picone, M.: Eighteenth Symposium (International) on Combustion, p. 1641, The Combustion Institute, 1981.
16. Strehlow, R.A.: Astro. Acta 15, 345, (1970).

17. Oran, E.S. and Boris, J.P.: Prog. Ener. Comb. Sci. 7, 1 (1981).

18. Boris, J.P. and Book, D.L.: Methods in Computational Physics, Vol. 16, p. 85, Academic Press, 1976. Also, Boris, J.P.: Flux-Corrected Transport Modules for solving Generalized continuity Equations, Naval Research Laboratory Memorandum Report 3237, 1976.

19. Book, D., Boris, J., Oran, E., Picone, M., Zalesak, S., and Kuhl, A., Seventh International Conference on Numerical Methods in Fluid Dynamics, Lecture Notes in Physics, 141, p. 84, Springer-Verlag, 1981. Also, Fry, M., Tittsworth, J., Kuhl, A., Book, D., Boris, J., and Picone, M.: Shock Capturing Using FLUX-Corrected Transport Algorithms with Adaptive Gridding, NRL Memorandum Report 4629, 1981.

20. Boris, J.P., Oran, E.S., Fritts, M.J. and Oswald, C.: Time Dependent, Compressible Simulations of Shear Flows: Tests of Outflow Boundary Conditions, NRL Memorandum Report 5249, 1983.

21. Strehlow, R.A. and Rubins, R.A.: AIAA J. 7, 1335 (1969).

22. Edwards, D.H. and Parry, D.J.: Astro. Acta 14, 533 (1969).

23. Edwards, D.H., Hooper, G. Job, E.M. and Parry, D.J.: Astro. Acta 15, 323 (1970).

24. Strehlow, R.A., Adamczyk, A.A. and Stiles, R.J.: Astro. Acta 17, 509 (1972).

25. Oppenheim, A.K. and Soloukhin, R.I.: Ann. Rev. Fluid Mech., Vol.5, 31 (1973).

26. Urtiew, P.A.: Acta. Astro. 3, 187 (1976).

FIGURE CAPTIONS

Figure 1. Composite of density contours from seven timesteps in the calculation of a propagating detonation in a hydrogen-oxygen-argon mixture in a 5 cm high tube. The direction of movement of the triple point is indicated by the lines with arrows.

Figure 2. Calculated paths of triple points for the same mixture as in Figure 1. (A) 5 cm high tube. (B) 7 cm high tube. (C) 9 cm high tube.

Figure 3. Temperature contours at six different times for the 5 cm tube calculation. The arrows indicate the direction of propagation of the triple points. The region between 1300 and 2100 K is shaded.

Figure 4. Pressure contours for the 5 cm tube calculation. The Mach stem, incident shock, and transverse waves are marked by M, I and TW, respectively.

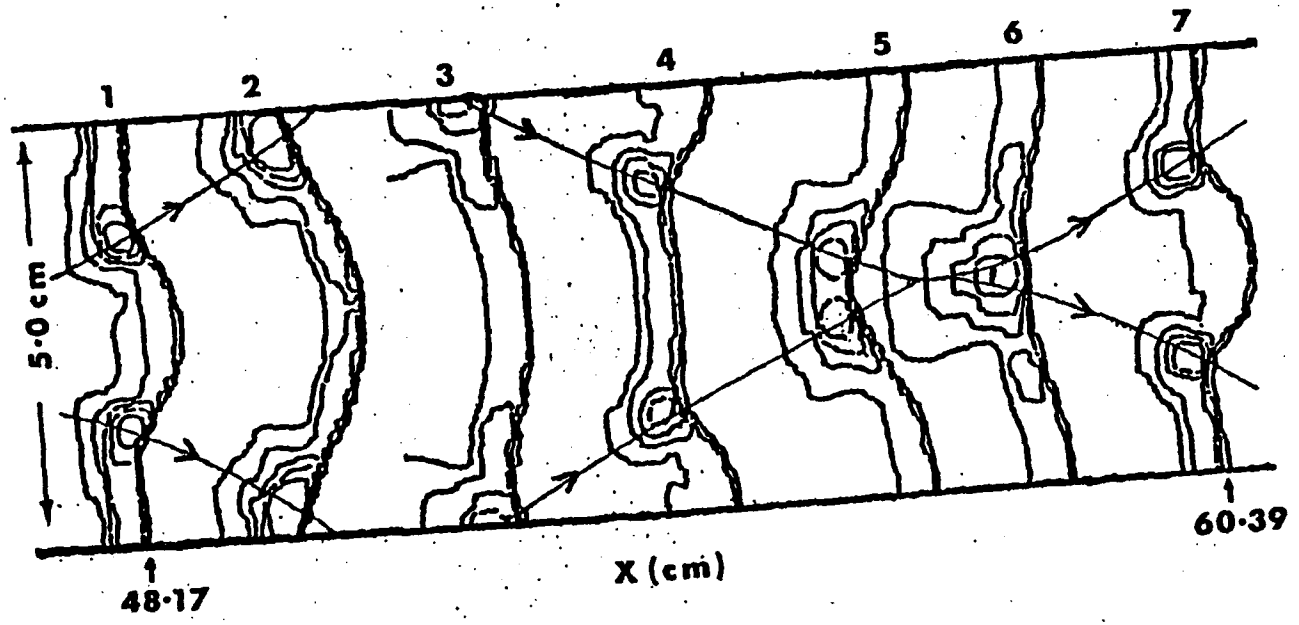

Figure 1

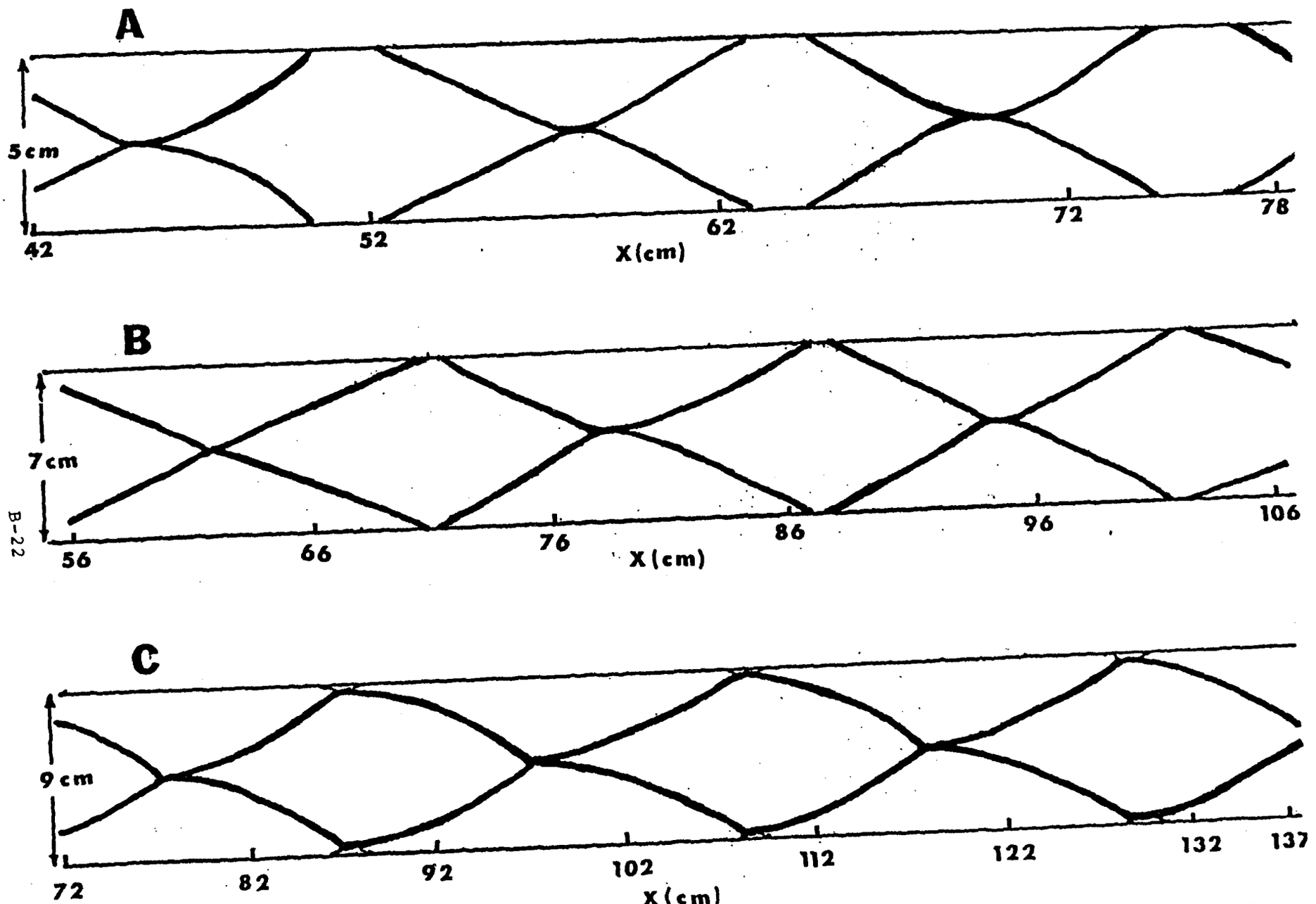
A
5cm
42
52
62
72
78
X(cm)
B
7cm
56
66
76
86
96
106
X(cm)
C
9cm
72
82
92
102
112
122
132
137
X(cm)

Figure 2

TEMPERATURE CONTOURS

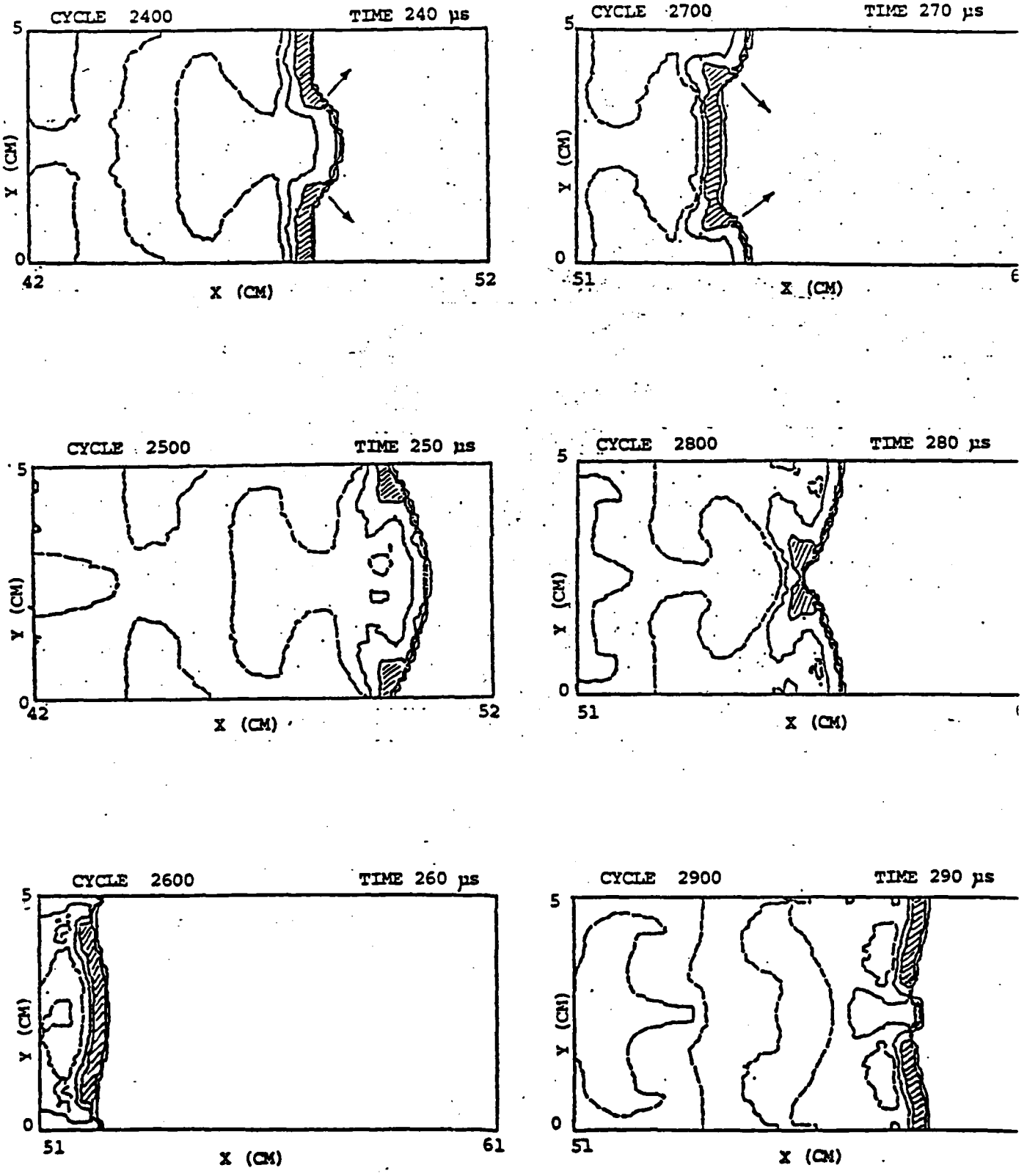

Figure 3

PRESSURE CONTOURS

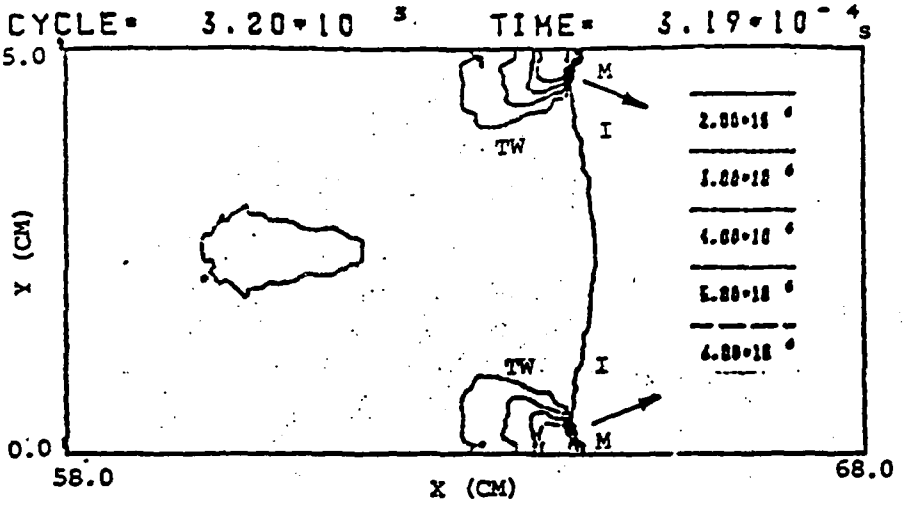

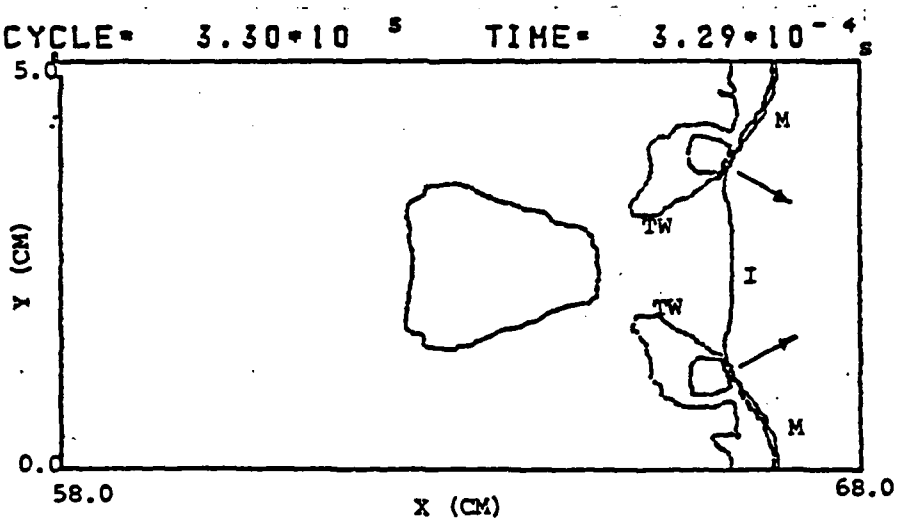

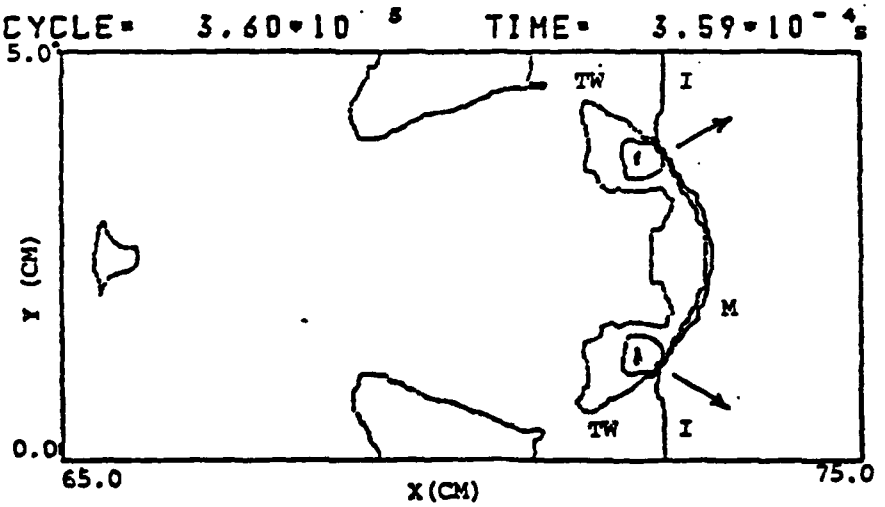

Figure 4

APPENDIX C

POWER-ENERGY RELATIONS FOR THE DIRECT INITIATION OF GASEOUS DETONATIONS

POWER-ENERGY RELATIONS FOR THE DIRECT INITIATION OF GASEOUS DETONATIONS

K. Kailasanath* and E.S. Oran

Laboratory for Computational Physics

Naval Research Laboratory

Washington, D.C. 20375

U.S.A.

* Science Applications, Inc. McLean, Virginia, U.S.A.

ABSTRACT

Recent studies on the direct initiation of gaseous detonations have shown that initiation depends not only on the energy deposited but also on the rate at which it is deposited, namely the power. In this paper, we have used a theoretical model to determine the relation between the power and the energy required for the initiation of planar, cylindrical and spherical detonations in a detonable gas mixture. The results from the model show that the qualitative differences in the power-energy relations obtained from two different experimental arrangements are due to differences in the geometry. We also show that the minimum power requirement corresponds to a shock of minimum Mach number only in the case of planar detonations. Finally, the effect on the power-energy relation of the ratio of specific heats and the experimental uncertainties in the determination of the induction times have been studied for an acetylene-oxygen-nitrogen mixture.

INTRODUCTION

The early studies of direct initiation of gaseous detonations* established the importance of the magnitude of the source energy. More recent studies‡ have shown the importance not only of the energy but also of the rate at which the energy is deposited, namely the power. The experimental results of Lee et al. (1975) indicate that there is a minimum detonation energy, E_m, below which a detonation would not occur no matter what the power is and that there is a minimum power, P_m, below which a detonation would not occur no matter what the total energy is. Later, they (Knystautas and Lee, 1976) noted that the requirement for a minimum value for the power of the source indicates that the source must be capable of generating a shock wave of certain minimum strength (Mach number). They also concluded that the minimum energy requirement implied that the shock wave must be maintained at or above this minimum strength for a certain minimum duration.

Recently these ideas have been used by Dabora (1980, 1982) to obtain a relation between the power and energy required for the direct initiation of hydrogen-air detonations in a shock tube. However, this power-energy relation is very different qualitatively from those of Knystautas and Lee (1976). More recently Abouseif and Toong (1982) have proposed a simple theoretical model to determine the power-energy relation and predict their respective threshold values. The predictions based on their model were in qualitative agreement with the experiments of Knystautas and Lee (1976).

*See Zeldovich et al. (1956), Litchfield et al. (1963) and Freiwald and Koch (1963).

‡See Oppenheim (1967), Bach et al. (1971), Meyer et al. (1973), Lee et al. (1975) and Knystautas and Lee (1976).

In this paper we have modified and extended the basic model proposed by Abouseif and Toong (1982) and have used it to determine the relation between the power and the energy required for the initiation of planar, cylindrical and spherical detonations in a detonable gas mixture. Specifically, we discuss its application to an acetylene-oxygen-nitrogen mixture. We have used the results from the model to explain the qualitative differences between the experimental results of Knystautas and Lee (1976) and Dabora (1980). The relation between the minimum power requirement and the Mach number of the shock wave has also been examined. Some of the limitations of the model are discussed, and several applications are described.

THE THEORETICAL MODEL

We can, in principle, study the direct initiation of detonations by performing detailed numerical simulations of the flow field generated by a given source of energy. In general, such a calculation is a complicated, multidimensional, multispecies, time-dependent problem. Part of the complication and cost of such calculations arises from the solution of the conservation equations, and part of it arises from integrating the large number of ordinary differential equations describing the chemical reactions. This latter factor is further complicated by the fact that we usually do not have an adequate representation of the chemical reactions with which to work. Thus, a convenient, inexpensive way to evaluate the relative tendency of different explosive mixtures to detonate would be very useful. Below we develop and expand a simple theoretical model proposed earlier by Abouseif and Toong (1982). Although this approach is not as precise as solving the full set of equations numerically, it offers a number of important insights and gets around the requirement of knowing the detailed chemical kinetics.

The model considers the flow generated by the motion of a constant velocity shock wave in planar, cylindrical and spherical geometries. As this shock wave passes through a gas mixture, the gas temperature and pressure increases. Due to this increase in temperature and pressure, ignition can occur in the shock heated gas mixture after the elapse of a certain time and this may lead to detonation.

A constant velocity shock wave can be formed in each of the three geometries by the motion of a constant velocity piston (Taylor, 1946; Kailasanath and Oran, 1983). Furthermore, it has been shown (Chu, 1955) that a pressure and velocity field identical to that ahead of a constant

velocity piston can be generated by appropriate energy addition. For example, a flow field bounded by a constant velocity planar piston and a constant velocity planar shock wave can be generated by a planar energy source with a constant rate of energy deposition. An example of such an energy source is the high pressure driver in a uniform shock tube. In general, the source power P_s required to generate a constant velocity piston in planar, cylindrical and spherical geometries can be written as (Abouseif and Toong, 1982; Kailasanath and Oran, 1983):

$$P_s(t) = \frac{\gamma}{(\gamma-1)} C_\alpha p_p u_p^\alpha t^{\alpha-1} \quad , \tag{1}$$

where $C_\alpha = 1, 2\pi, 4\pi$ for $\alpha = 1,2,3$ corresponding to the planar, cylindrical and spherical geometries respectively; p_p and u_p are the pressure and velocity at the piston surface and t is the duration of energy deposition. The energy deposited is given by the time integral of the power, that is

$$E_s(t) = \frac{\gamma}{(\gamma-1)} \frac{C_\alpha}{\alpha} p_p u_p^\alpha t^\alpha \quad . \tag{2}$$

Equations (1) and (2) give the source power and the source energy required to generate a constant velocity piston in the three geometries. As shown elsewhere (Kailasanath and Oran, 1983), if the piston velocity is steady, a constant velocity shock wave could be generated ahead of it. If the piston velocity is reduced (by altering the energy deposition rate), rarefaction waves will be generated ahead of it and these, on catching up

with the shock wave , will reduce the shock velocity. However if the shock has been in motion for a sufficiently long time, chemical reactions would begin in the shock heated gas mixture. Then, even if the piston decelerates and produces rarefaction waves, these will have very little effect on the motion of the shock. In this case we could have a detonation.

Let us call the minimum time of shock travel required to initiate a detonation t_{cr}. Using this in Eqs. (1) and (2), we have

$$(E_s)_{cr} = \frac{\gamma}{(\gamma-1)} \frac{C_\alpha}{\alpha} p_p u_p^\alpha t_{cr}^\alpha \quad . \tag{3}$$

and

$$(P_s)_{cr} = \frac{\gamma}{(\gamma-1)} C_\alpha p_p u_p^\alpha t_{cr}^{\alpha-1} \quad . \tag{4}$$

In the planar case, the pressure p_p and fluid velocity u_p at the piston surface are the same as those just behind the shock. However, in the cylindrical and spherical cases, the flow field between the shock and the piston surface is nonuniform and can be obtained by solving the governing partial differential equations. However, the solution procedure is considerably simplified if we seek a similarity solution. Then the system of partial differential equations can be reduced to a system of coupled ordinary differential equations:

$$\frac{(u-L)}{\rho} \frac{d\rho}{dL} + \frac{du}{dL} + (\alpha-1) \frac{u}{L} = 0 \tag{5}$$

$$(u-L)\frac{du}{dL} = -\frac{1}{\rho}\frac{dp}{dL} \qquad (6)$$

$$\frac{dp}{dL} = \frac{\gamma p}{\rho}\frac{d\rho}{dL} \quad . \qquad (7)$$

In the above system of equations, the density ρ, the velocity u and the pressure p are all functions of the similarity variable L, which is equal to the radial location r divided by the time t. The pressure and the velocity at the piston surface which are required in Eqs. (3,4) can be obtained by solving Eqs. (5-7) in the following manner. For a shock of a given Mach number, we can calculate the flow condition just behind the shock using normal shock relations. We can then integrate Eqs. (5-7) from just behind the shock to the piston surface to obtain P_p and u_p which are needed in Eqs. (3,4). The procedure is further simplified by appropriately combining Eqs. (5-7) into two equations and normalizing them. This is discussed in detail elsewhere (Kailasanath and Oran, 1983).

In order to determine the power-energy relation using Eqs. (3,4) we also need to know t_{cr}. This time must at least be equal to the time at which ignition first occurs in the flow field (Abouseif and Toong, 1982). As noted by Urtiew and Oppenheim (1967), ignition usually occurs first at the contact surface (i.e., at the piston surface here) since the temperature and pressure is highest at this location. So a first estimate of the time t_{cr} would be the induction delay time corresponding to the conditions at the piston surface.

RESULTS AND DISCUSSION

We have used the model described above to determine the power-energy relations for the initiation of planar, cylindrical, and spherical detonations in an acetylene-oxygen-nitrogen mixture. The initial temperature and pressure of the mixture were taken to be 300 K and 100 torr (0.1316 atm) to correspond to the initial conditions in the experiments of Knystautas and Lee (1976). As a first approximation, the time duration necessary for successful initiation was assumed to be equal to the chemical induction time of the mixture corresponding to the conditions at the piston surface.

The critical source power given by Eq. (4) is time dependent for the cylindrical and spherical cases. In order to relate the critical source energy to a critical source power, we need to define an average or "effective" power. Following Abouseif and Toong (1982), we define an average critical source power as

$$(P_s)_{av} = \frac{(E_s)_{cr}}{t_{cr}}. \qquad (8)$$

This power also corresponds to the critical peak averaged power of the source as defined by Knystautas and Lee (1976). For the discussion below, we have used the terms power and energy to refer to the average critical source power (Eq. (8)) and the critical source energy (Eq. (3)).

Cylindrical Detonations in an Acetylene-Oxygen-Nitrogen Mixture

We have determined the power-energy relation for the initiation of cylindrical detonations using Eqs. (3) and (8). The induction time data used

were those obtained by Edwards et al. (1981) for an acetylene-oxygen-nitrogen (2:5:4) mixture and are given by:

$$Log\ (\tau[O_2]) = -9.41\ (\pm\ 0.2) + \frac{71.35\ (\pm\ 3.34)}{19.14\ T} \qquad (9)$$

where τ is the induction time in seconds, $[O_2]$ is the concentration in mol/liter, and T is the temperature in thousands of degrees K. Three different power-energy relations obtained from the theoretical model are shown in Figure 1. Curve A was obtained by using the smallest value of the induction time given by Eq. (9), that is, by choosing the negative signs. Curve B was obtained by using the mean values and curve C by using the largest value of the induction time (by choosing the positive signs). The arrows on curve C indicate the direction of increasing Mach number. First, we note that each curve has a minimum power and a minimum energy. We also observe that as the Mach number decreases below the Mach number corresponding to the minimum power, both the average source power and the source energy increase. However, when the Mach number increases above the Mach number corresponding to the minimum power, the energy first decreases to the minimum energy and then increases again. All three curves exhibit these same qualitative trends.

The shape of these curves can be explained in the following manner. As the Mach number of the shock wave decreases, the pressure and the temperature behind it decrease. This decrease also results in a decrease of the pressure and velocity at the piston surface. This would tend to decrease both the power and the energy since, as seen in Eqs. (1,2),

$$p \sim p_p u_p^2 t \qquad (10)$$

$$E \sim p_p u_p^2 t^2 \qquad (11)$$

This tendency is, however, opposed by the tendency of the induction time to increase with decreases in the pressure and the temperature. For low Mach numbers, (i.e., low temperatures behind the shock) a small decrease in the Mach number of the shock wave leads to a large increase in the induction time. The shape of the curves in Figure 1 implies that this increase in induction time is more than sufficient to compensate for the decrease in the pressure and the velocity for Mach numbers below that corresponding to the minimum power. Therefore both the power and the energy increase with decreasing Mach number. Since the energy is proportional to the product of the power and the induction time (Eqs. (10,11)), the energy increases faster with induction time than the power does. As the Mach number increases above that corresponding to the minimum power, the increase in the pressure and velocity is larger than the decrease in the induction time. Therefore the power increases. However, for a certin range of Mach numbers, the increase in the pressure and velocity is not sufficient to compensate for the decrease in the square of the induction time. Therefore the energy decreases until it attains a minimum value, even though the power increases. Finally, for Mach numbers above that corresponding to the minimum energy, the increase in the pressure and velocity are easily able to overcome the decrease in the induction time with increasing Mach number and both the power and the energy increase. This occurs because the rate of decrease of the induction time with temperature is small for high temperatures (i.e., high Mach numbers) according to Eq. (9).

The power-energy curve obtained using data from the spark ignition experiments of Knystautas and Lee (1976) has also been included in Figure 1 as curve D. The data for curve D is the same as that used by Abouseif and

Toong (1982) for their Figure [1], and was originally presented in Figure [4] of Knystautas and Lee (1976). Curve D exhibits the same qualitative trends as those of the theoretical curves discussed above. However, we observe that the values of the minimum power and the minimum energy from the four curves are very different from each other. The differences in the values of these parameters from the three "theoretical" curves (A,B, and C) indicate that the experimental uncertainties in the values of the induction times used have a significant effect on the value of the minimum power and the minimum energy. The minimum power varies from about 0.3 MW/cm to about 1 MW/cm and the minimum energy varies from about 0.012 J/cm to about 0.1 J/cm. The experimentally determined minimum power (from curve D) is about 0.13 MW/cm, which is lower than the calculated values, and the minimum energy is about 0.1 J/cm, which is at the top of the range of calculated values.

The quantitative differences between the experimental and theoretical values could be due to a variety of factors, a few of which we now discuss. As observed from curves A, B, and C, uncertainties in the induction time data can have a significant effect on the values of the minimum power and the minimum energy. Expressions such as Eq. (9) for the induction time are obtained by fitting to a limited range of experimental data. However, here we have used Eq. (9) for a range of temperatures and pressures far greater than that over which it was determined. Furthermore, for obtaining the theoretical results, we had assumed a constant value of 1.2 for γ, the ratio of specific heats. For high Mach numbers, the γ of the shocked gas could be very different from that ahead of the shock wave because of the large temperature difference across the shock wave. The effect of γ on the power-energy relations is discussed below.

Effect of γ on Power-Energy Relations

The power-energy calculations were repeated using different values for γ and the results are shown as curves A and C in Figures 2 and 3. In Figure 2, the average source power is shown as a function of the shock Mach number and in Figure 3, the source energy is shown as a function of the shock Mach number. From these figures, we observe that γ does indeed have a significant effect on the minimum power and the minimum energy. When γ is changed from 1.1 to 1.4, the minimum source power decreases from 2.0 MW/cm to 0.18 MW/cm and the minimum energy decreases from 0.065 to about 0.02 J/cm. The Mach number at which the shock must travel to attain the minimum power is also very different, as seen in Figure 2. Changing γ from 1.4 to 1.1 doubles the Mach number corresponding to the minimum power from 8 to 16. The effect of γ on the power-energy relation arises partly from the factor $(\gamma/\gamma-1)$ in Eqs. (3) and (4) and partly from the fact that the temperature behind a shock of given Mach number is very different for different γ's.

The effect of the factor $(\gamma/\gamma-1)$ is to change quantitatively the values of the source power and the source energy corresponding to the shock of a given Mach number and is the same for all Mach numbers. The changes in the temperature behind a shock wave due to assumed differences in γ is, however, a function of the shock Mach number. Let us consider a shock wave of the Mach number 10. In Table 1 we have given the pressure ratio, the temperature ratio and the temperature behind this shock wave for different values of γ. We have also included the case where γ is different across the shock wave as case 3. For obtaining case 3, we have re-derived the normal shock relations but with variable γ across the shock wave. The derivation of these "modified" shock relations has been presented in detail elsewhere

(Kailasanath and Oran, 1983). We see that for Case 3, the temperature behind the shock wave is significantly lower than that for case 2. Case 3 is a more realistic case than case 2, since γ is generally lower behind the shock. However, the appropriate γ for conditions behind the shock wave is different for different Mach numbers, since the temperatures are different. Thus a better approach is first to guess a γ for each Mach number and use it to calculate the temperature behind the shock. This new temperature implies a new γ. Using this new γ in the modified shock relations we get a new temperature. This iterative procedure is continued till convergence is achieved.

The power-energy calculations were repeated using the correct γ (as described above) and the results are presented as curve B in Figures 2 and 3. For low Mach numbers, curve B lies close to curve A and for very high Mach numbers it tends towards curve C. This is not surprising since for the acetylene-oxygen-nitrogen mixture being studied here, γ varies from 1.31 to 1.16 when the Mach number changes from 2 to 24. From curve B in Figures 2 and 3 we also note that the minimum power and the minimum energy conditions occur at Mach number of 10.0 and 15.5 respectively.

From the above discussion it is clear that the effect of using the correct γ is mainly to alter the Mach number corresponding to the minimum power and the minimum energy condition. However, the calculated values of the minimum power and the minimum energy are still different from those obtained experimentally. Therefore we examine another possible reason for the differences between the experimental and the theoretical values: the uncertainty in the appropriate time to be used for t_{cr} in Eqs. (3) and (8).

Critical Time for Energy Deposition

As a first approximation, we assumed that energy must be deposited until ignition occurs at some point in the flow field between the shock and the piston surface. Since, in general, the temperature and pressure is highest at the piston surface, we used the chemical induction time corresponding to these conditions as the appropriate time for energy deposition. However, when there is fluid motion, ignition can occur before the time corresponding to the constant volume, homogeneous chemical induction time. For example, for a certain range of temperatures and pressures, oxy-hydrogen mixtures with small perturbations could have significantly reduced ignition times. The specific effect of this phenomenon on the power-energy relations will be reported in a subsequent paper. In gas mixtures which are not particularly sensitive to perturbations, the shortest induction time in the shocked region seems to be the necessary condition for the initiation of detonations. However, we need to consider whether this is a sufficient condition also.

Shock tube simulations have indicated that the time at which a detonation wave is first observed is only very slightly longer than the time at which ignition first occurs. That is, the time between ignition and the formation of a detonation wave is small when compared to the induction time. This is not surprising when we consider the fact that for many reactive systems, the reaction time is very small compared to the induction time. The results of Abouseif and Toong (1982) on the initiation of planar detonations also supports this observation. However we have not studied the effect of geometry on the time between ignition and detonation. It could very well be that due to the volume change in spherical and cylindrical geometries, this time is significant when compared to the induction time. This needs to be

studied before one can confidently use the induction time as the appropriate time for t_{cr}.

We have compared the results from the theoretical model for the case of cylindrical detonations with the experimental results of Knystautas and Lee (1976) because in both cases the amount of energy deposited was proportional to the second power of the time. However, it is important to note that in the theoretical model we have considered only constant velocity shock waves and it was this that made it possible to assign a single induction time to each shock wave. If the velocity of the shock wave is not constant, it is not possible to assign a single induction time to it since the flow field behind the shock wave would be time-dependent. Thus, shock waves of different time histories can deposit the same amount of energy but at different average source powers. This could be an imporant factor in the quantative differences between the experimental and theoretical values.

Initiation of Planar Detonations

The derived power-energy relation for the initiation of planar detonations in the same oxy-acetylene mixture is shown in Figure 4. In this figure, we also show the shock tube data of Dabora (1980) on the direct initiation of detonations in a stoichiometric hydrogen-air mixture. The point to notice is that both curves exhibit the same qualitative behavior. Unlike the cylindrical case, each value of the power corresponds to an unique value of energy. The direction of increasing shock strength (as determined by the Mach number) is also shown in Figure 4. In the planar case, we see that as the Mach number decreases the power always decreases. As noted earlier in the cylindrical case, as the Mach number decreases, the power

decreases only up to the minimum power. Then the power increases with a decrease in the Mach number of the shock wave. Therefore, the qualitative difference in the experimental data of Knystautas and Lee (shown in Figure 1) and Dabora (shown in Figure 4) are due to the difference in the geometry of the two experiments.

We also observe in Figure 4 that as the Mach number decreases, we need more and more energy to initiate a detonation. The trend of the curves indicates that there is a minimum Mach number below which a detonation will not occur (i.e., would require an infinite amount of energy). The value of the power corresponding to this minimum Mach number is the minimum power. This agrees with the observation made by Knystautas and Lee (1976) that the requirement for a minimum value of the source power indicates that the source must be capable of generating a shock wave of a certain minimum Mach numb r. However, we observe from Figure 1 (see also Figure 2) that for the case of cylindrical detonations, the minimum power does not correspond to the shock wave of minimum Mach number. In the cylindrical case, it is possible to initiate a detonation with a shock wave of lower Mach number than that corresponding to the minimum power. Such a shock will have to be maintained for a longer time than the shock corresponding to the minimum power and hence will require a larger amount of energy.

Initiation of Spherical Detonations

The power-energy curve for the initiation of spherical detonations is similar to the curve for the cylindrical case. However, for the case of spherical detonations, the power is

$$P \sim p_p u_p^3 t^2, \tag{12}$$

but the energy is still

$$E \sim P\,t. \tag{13}$$

Since the power and energy are proportional to higher powers of the time, t, uncertainties in t will have a greater effect on the value of the minimum power and the minimum energy. Further work is being carried out currently to study the initiation of spherical detonations in hydrogen-air mixtures and to compare this to experimental data.

SUMMARY AND CONCLUSIONS

In this paper we have used a theoretical model to determine the relation between the power and the energy required for the initiation of planar, cylindrical and spherical detonations in a gas mixture. The results discussed above show that though the simple theoretical model has significant limitations, it can still be used to explain the qualitative differences in the power-energy relations obtained from different experimental arrangements. Another result from the model is that the minimum power requirement corresponds to a shock of minimum Mach number only in the case of planar detonations.

The results from the model on the initiation of cylindrical detonations in an acetylene–oxygen–nitrogen mixture qualitatively agree with experimental data. Some of the reasons for the quantitative differences have been examined. One of the important parameters in the model is the critical time for energy deposition. This time is related to the induction time and the results presented above show that uncertainties in the induction time data used can have a significant effect on the power-energy relations. The results also indicate that further work needs to be done to determine the effect of the geometry on the critical time for energy deposition.

The quantitative differences between the experimental and theoretical results may also arise because of the model assumption that the velocities of the shock waves are constant. This may not be so in the experiments. Furthermore, the model considers only the minimum power and energy required to initiate a detonation wave. We have not examined whether this would result in a self-sustained, propagating detonation wave. Detonation propagation is characterized by complicated interactions among incident shock

waves, transverse waves and Mach stems which form detonation cells. These must be described by multidimensional theories and simulations. The results from such studies need to be considered to extend the work presented here to the study of self-sustained detonation waves.

One application of the model presented here is to determine the relative tendency of different explosives to detonate, since the limitations of the model would then be less critical. This would be particularly useful for studying the effect of additives on the detonability of condensed phase explosives. Further work is being carried out to modify the model for such applications.

Acknowledgements

The authors greatfully acknowledge suggestions, useful conversations with, and help from Jay P. Boris and T.R. Young. The authors also acknowledge the editorial assistance of Ms. F. Rosenberg. This work has been supported by the Office of Naval Research through the Naval Research Laboratory.

REFERENCES

Abouseif, G.E. and Toong, T.Y. (1982) On Direct Initiation of Gaseous Detonations. Combust. Flame 45, 39-46.

Bach, G.G., Knystautas, R. and Lee, J.H. (1971) Initiation Criteria for Diverging Gaseous Detonations. Thirteenth Symposium (International) on Combustion, The Combustion Institute, Pittsburgh, PA, pp. 1097-1110.

Chu, B.T. (1955) Pressure Waves Generated by Addition of Heat in a Gaseous Medium. NACA TN 3411, NACA, Washington, DC, 47 pp.

Dabora, E.K. (1980) Effect of Additives on the Lean Detonation Limit of Kerosene Sprays. UCONN0507-129-F, The University of Connecticut, Storrs, CT, 46 pp.

Dabora, E.K. (1982) The Relation between Energy and Power for Direct Initiation of Hydrogen-Air Detonations. Presented at the Second International Workshop on the Impact of Hydrogen on Water Reactor Safety, Albuquerque, NM.

Edwards, D.H., Thomas, G.O. and Williams, T.L. (1981)Initiation of Detonation by Steady Planar Incident Shock Waves. Combust. Flame 43, 187-198 .

Freiwald, H. and Koch, H.W. (1963) Spherical Detonations of Acetylene-Oxygen-Nitrogen Mixtures as a Function of Nature and Strength of Initiation. Ninth Symposium (International) on Combustion, Academic Press, New York, NY, pp. 275-281.

Kailasanath, K. and Oran, E.S. (1983) The Relation between Power and Energy in the Shock Initiation of Detonations - I. NRL Memorandum Report, Naval Research Laboratory, Washington, DC (to be published).

Knystautas, R. and Lee, J.H. (1976) On the Effective Energy for Direct Initiation of Gaseous Detonations. Combust. Flame 27, 221-228.

Lee, J.H., Knystautas, R. and Guirao, C.M. (1975) Critial Power Density for Direct Initiation of Unconfined Gaseous Detonations. Fifteenth Symposium (International) on Combustion, The Combustion Institute, Pittsburgh, PA, pp. 53-67.

Litchfield, E.L., Hay, M.H. and Forshey, D.R. (1963) Direct Electrical Initiation of Freely Expanding Gaseous Detonation Waves. Ninth Symposium (International) on Combustion, Academic Press, New York, NY, pp. 282-286.

Meyer, J.W., Cohen, L.M. and Oppenheim, A.K. (1973) Study of Exothermic Processes in Shock Ignited Gases by the use of Laser Shear Interferometry. Combust. Sci. Tech. 8, 185-197.

Oppenheim. A.K. (1967) The No-Man's Land of Gasdynamics of Explosions. Appl. Mech. Rev. 20, 313-319.

Taylor, G.I. (1946) The Air Wave Surrounding an Expanding Sphere. Proc. Roy. Soc. (London), A 186, 273-292.

Urtiew, P.A. and Oppenheim, A.K. (1967) Detonative Ignition Induced by Shock Merging. Eleventh Symposium (International) on Combustion, The Combustion Institute, Pittsburgh, PA, pp. 665-670.

Zeldovich, Y.B., Kogarko, S.M. and Simonov, N.N. (1956) An Experimental Investigation of Spherical Detonation of Gases. Soviet Phys.-JETP 1, 1689-1713.

TABLE HEADING

Table 1. Effect of the Ratio of Specific Heats

CASE	γ_o [a]	γ_s	p_s/p_o	T_s/T_o	T_s
1	1.2	1.2	109.000	10.900	3270.0
2	1.3	1.3	112.913	15.710	4712.89
3	1.3	1.2	118.426	11.454	3436.26

(a) The conditions ahead of the shock wave are denoted by "o" and those behind by "s".

FIGURE CAPTIONS

Figure 1. Power-energy relations for the initiation of cylindrical detonations in an acetylene-oxygen-nitrogen mixture (2:5:4) at 0.1316 atm and 300K. . The data for curve D was obtained from spark ignition experiments (Knystautas and Lee, 1976). Curves A, B, and C are explained in the text. The arrows on Curve C indicate the direction of increasing Mach number.

Figure 2. The average source power as a function of the shock Mach number. Curves A and C were obtained assuming γ to be constant across the shock wave. Curve B was obtained assuming γ to be variable as explained in the text.

Figure 3. The source energy as a function of the shock Mach number. Curves A and C were obtained assuming γ to be constant across the shock wave. Curve B was obtained assuming γ to be variable as explained in the text.

Figure 4. Power-energy relations for the initiation of planar detonations. The x's are data obtained from shock tube experiments (Dabora, 1980).

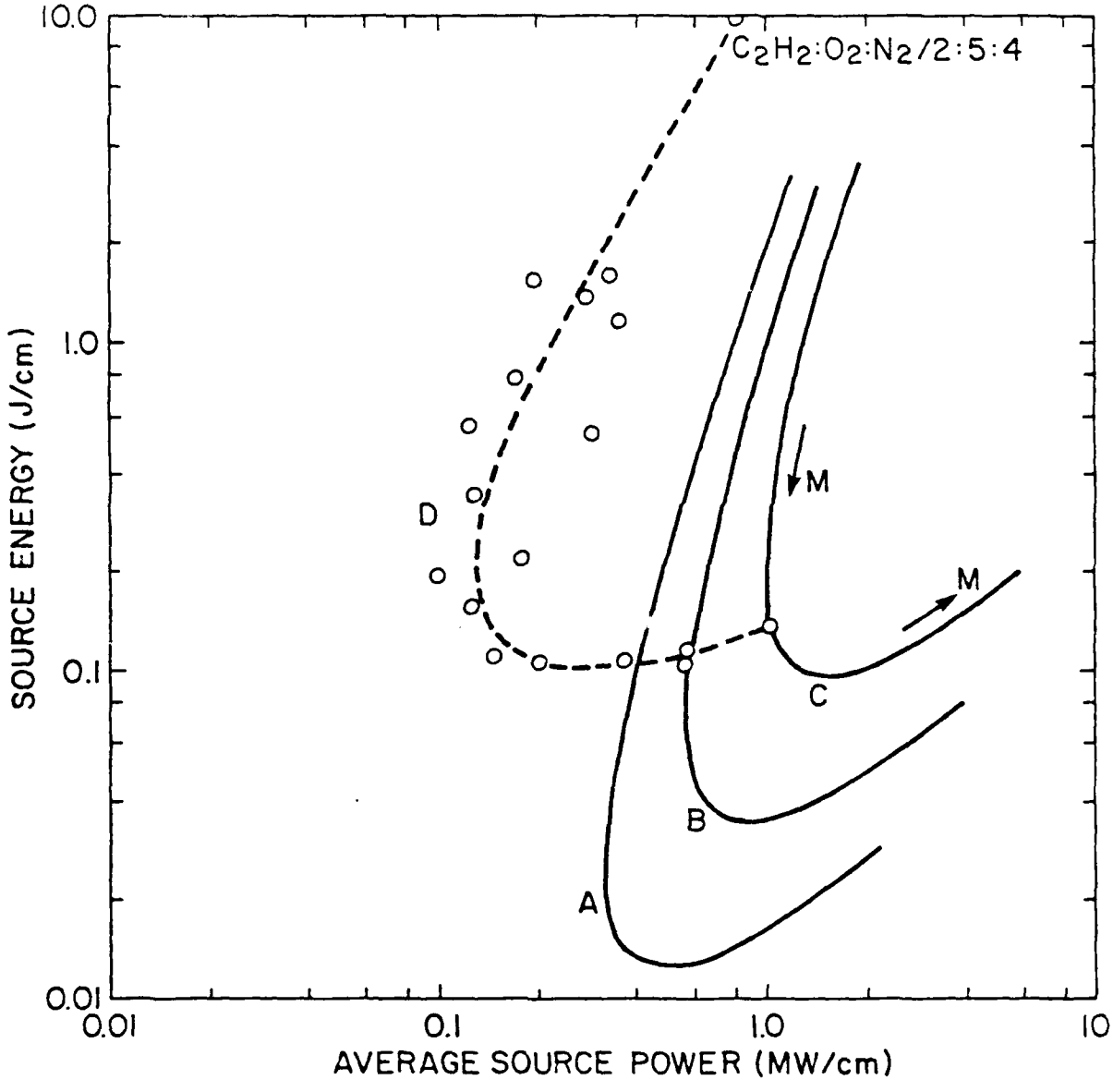
10.0
1.0
0.1
0.01
0.01
0.1
1.0
10
SOURCE ENERGY (J/cm)
AVERAGE SOURCE POWER (MW/cm)
$C_2H_2:O_2:N_2/2:5:4$
D
M
M
C
B
A

Figure 1

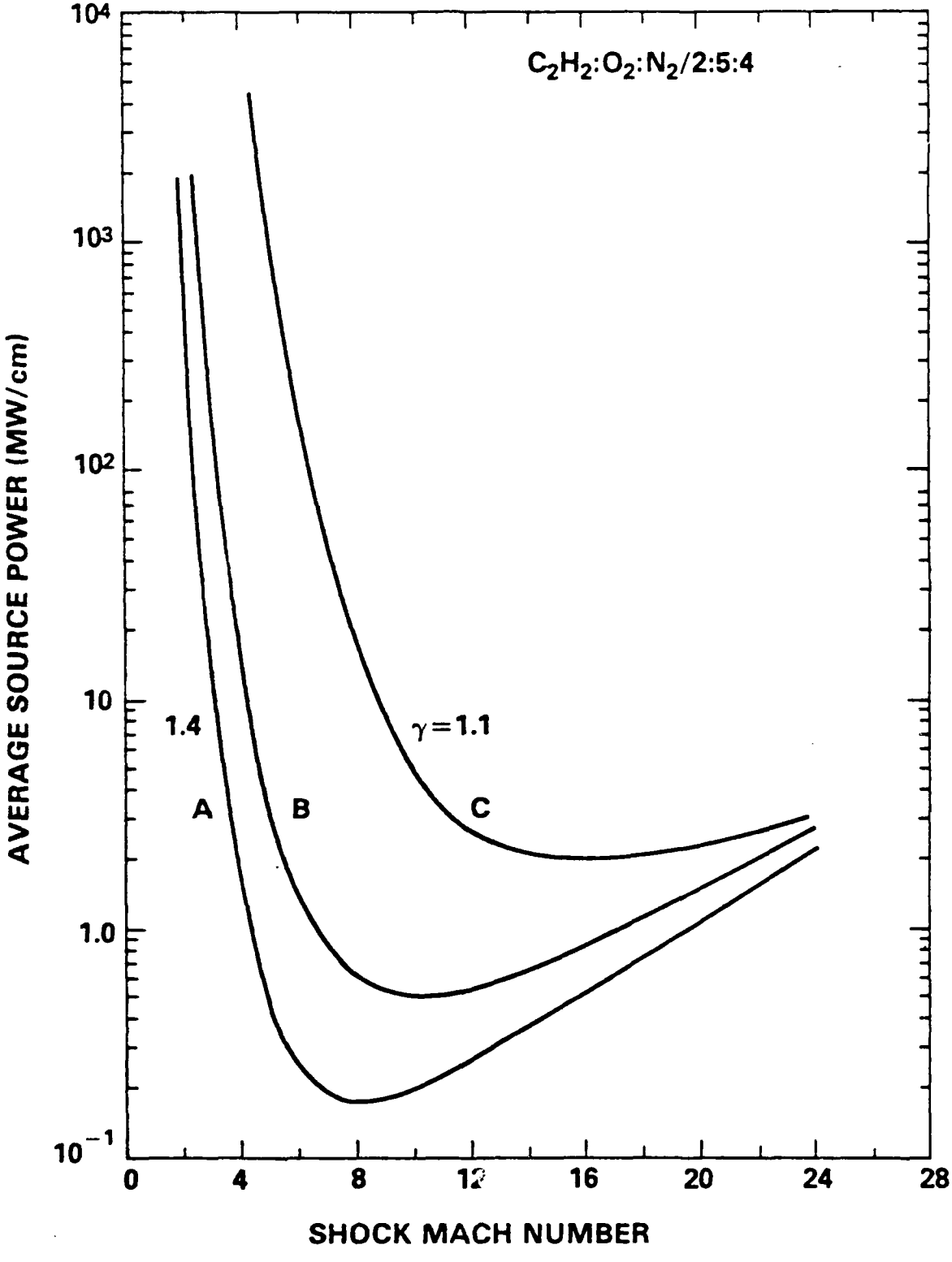
$C_2H_2:O_2:N_2$/2:5:4
AVERAGE SOURCE POWER (MW/cm)
SHOCK MACH NUMBER
10^4
10^3
10^2
10
1.0
10^{-1}
0
4
8
12
16
20
24
28
1.4
$\gamma=1.1$
A
B
C

Figure 2

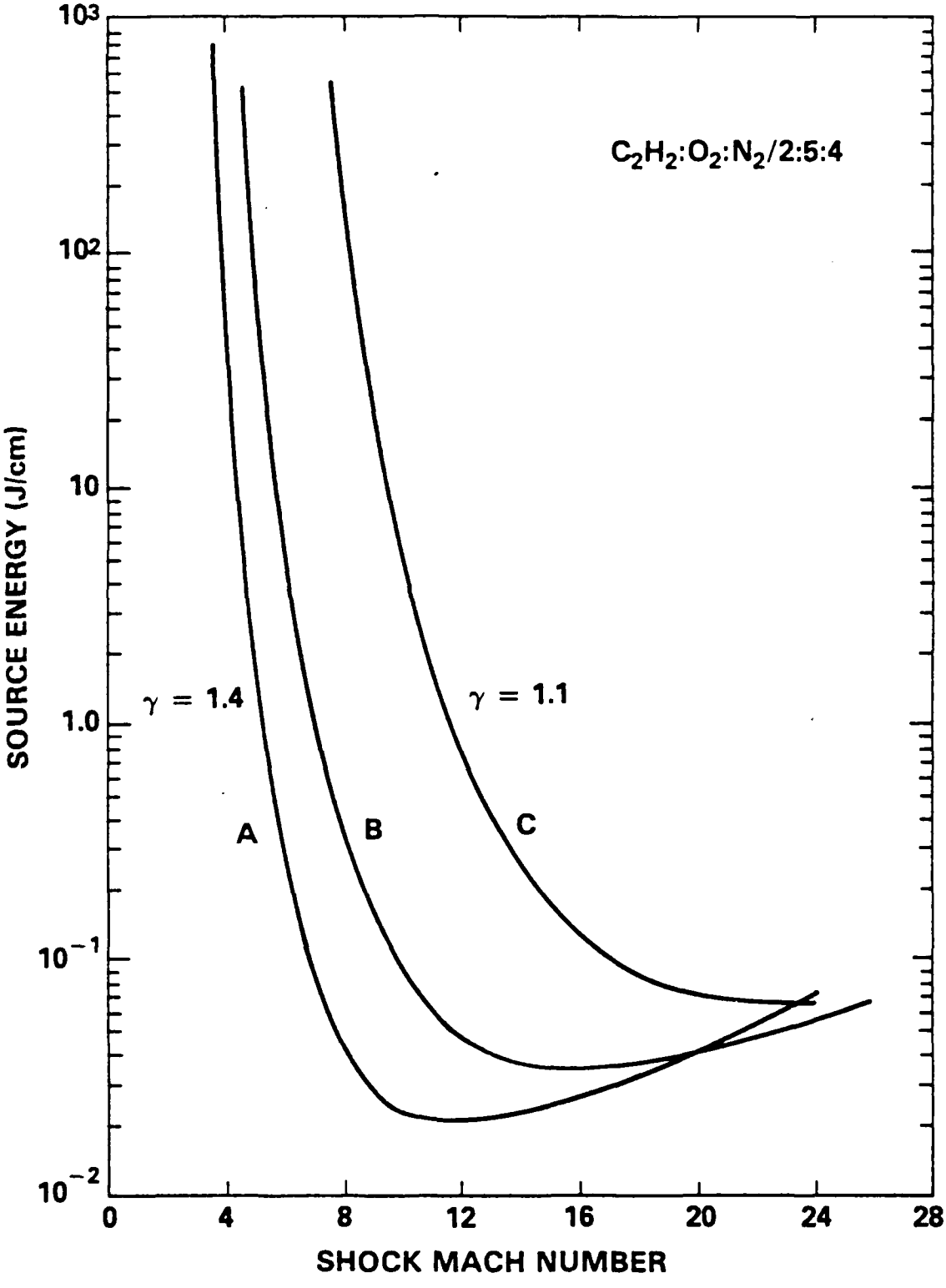
10^3
10^2
10
1.0
10^{-1}
10^{-2}
SOURCE ENERGY (J/cm)
$C_2H_2:O_2:N_2/2:5:4$
$\gamma = 1.4$
$\gamma = 1.1$
A
B
C
0
4
8
12
16
20
24
28
SHOCK MACH NUMBER

Figure 3

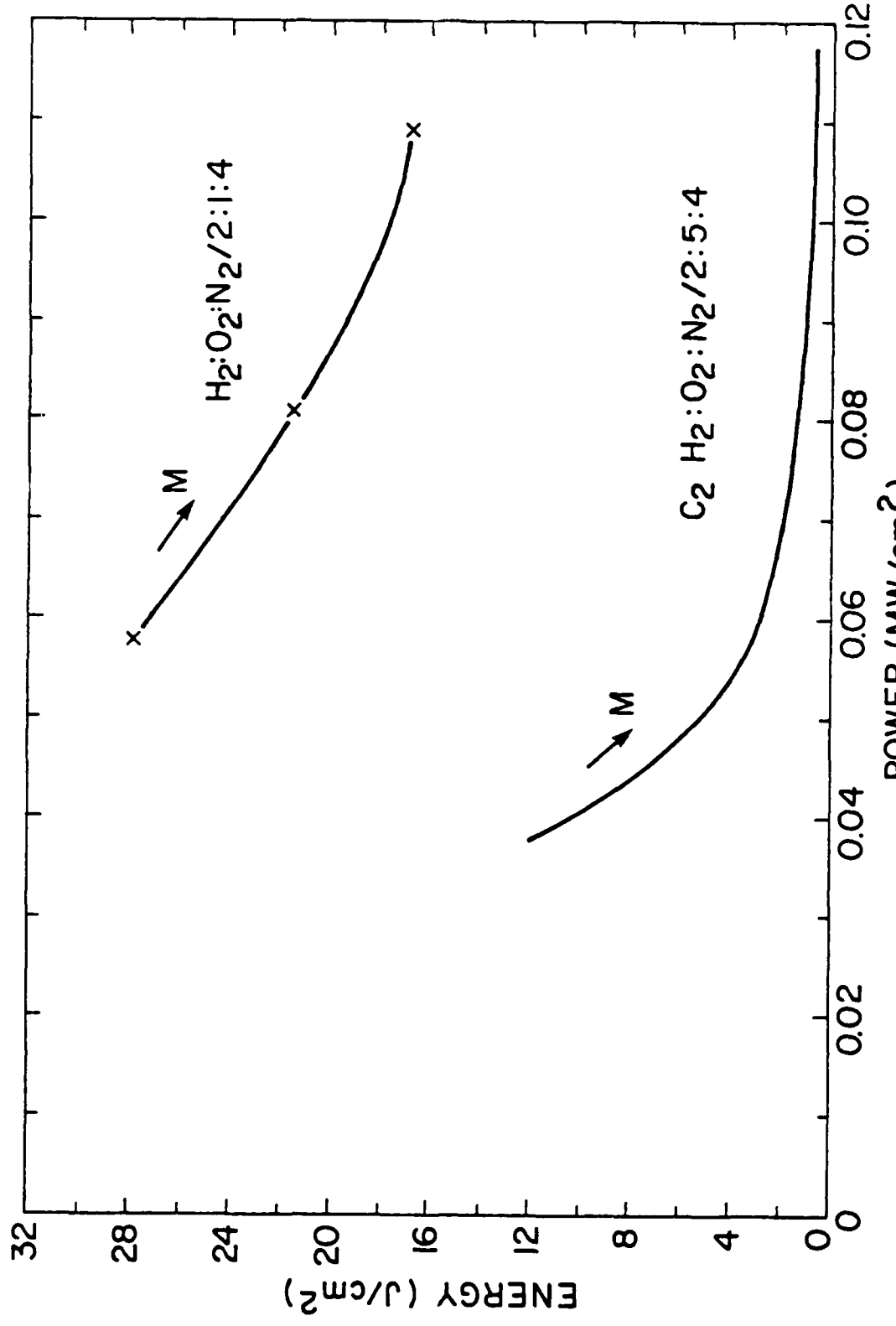
ENERGY (J/cm²)
POWER (MW/cm²)
0
4
8
12
16
20
24
28
32
0.02
0.04
0.06
0.08
0.10
0.12
M
H₂:O₂:N₂/2:1:4
M
C₂ H₂:O₂:N₂/2:5:4

Figure 4

APPENDIX D

SHOCK INITIATION OF DETONATIONS IN HYDROGEN-AIR MIXTURES

SHOCK INITIATION OF DETONATIONS IN HYDROGEN-AIR MIXTURES

K. Kailasanath*, E.S. Oran, T.R. Young and J.P. Boris
Laboratory for Computational Physics
Naval Research Laboratory
Washington, DC 20375

*Science Applications, Inc. McLean, Virigina

Background

A simple theoretical model was developed to determine the relation between the power and energy required for the shock initiation of gaseous detonations [1]. The model successfully explained the qualitative differences in the power-energy relations obtained from two different experimental arrangements [2]. The model also gave qualitatively good predictions of the power-energy relation for the initiation of cylindrical detonations in an acetylene-oxygen-nitrogen mixture [2]. However, the minimum power and the minimum energy predicted by the model were quantitatively different from those obtained experimentally. One reason for the difference is the uncertainty in the appropriate time to be used for the critical time for which energy must be deposited in order to initiate a detonation [1]. In this paper we address this issue in some detail by comparing the results from the simple theoretical model to those obtained from detailed numerical simulations on the initiation of planar detonations in an hydrogen-air mixture.

The Theoretical Model

The model, based on one developed earlier by Abouseif and Toong [3], considers the flow generated by the motion of a constant velocity shock wave in planar, cylindrical and spherical geometries. As this shock wave passes through a gas mixture, the gas temperature and pressure increases. Due to this increase in temperature and pressure, ignition can occur in the shock heated gas mixture after the elapse of a certain time and this may lead to detonation.

A constant velocity shock wave can be formed in each of the three geometries by the motion of a constant velocity piston [4,1]. Furthermore it can be shown [5] that a pressure and velocity field identical to that ahead of a constant velocity piston can be generated by appropriate energy addition. For example, a flow field bounded by a constant velocity planar shock wave and a constant velocity planar piston can be generated by a planar energy source with a constant rate of energy deposition. An example of such an energy source is the high pressure driver in a uniform shock tube. In general, the source power required to generate a constant velocity piston in planar, cylindrical and spherical geometries can be written as [1,3]:

$$P_s(t) = \frac{\gamma}{(\gamma-1)} C_\alpha p_p u_p^\alpha t^{\alpha-1} \quad , \qquad (1)$$

where C_α = 1, 2π, 4π for α = 1, 2, 3 corresponding to the planar, cylindrical and spherical geometries respectively; p_p and u_p are the pressure and velocity at the piston surface and t is the duration of energy deposition. The energy deposited is given by the time integral of the power, that is

$$E_s(t) = \frac{\gamma}{(\gamma-1)} \frac{C_\alpha}{\alpha} p_p u_p^\alpha t^\alpha \quad . \tag{2}$$

Equations (1) and (2) give the source power and the source energy required to generate a constant velocity piston in the three geometries. If the piston velocity is steady, a constant velocity shock wave could be generated ahead of it [1]. If the piston velocity is reduced, rarefaction waves will be generated ahead of it and these, on catching up with the shock wave, will reduce the shock velocity. However if the shock has been in motion for a sufficiently long time, chemical reactions can begin in the shock heated gas mixture. Then, even if the piston decelerates and produces rarefaction waves, these will have very little effect on the motion of the shock. In this case we have a detonation.

Let us call the minimum time of shock travel required to initiate a detonation t_{cr}. Using this in Eqs. (1) and (2), we have

$$(P_s)_{cr} = \frac{\gamma}{(\gamma-1)} C_\alpha p_p u_p^\alpha t_{cr}^{\alpha-1} \quad , \tag{3}$$

and

$$(E_s)_{cr} = \frac{\gamma}{(\gamma-1)} \frac{C_\alpha}{\alpha} p_p u_p^\alpha t_{cr}^\alpha \quad . \tag{4}$$

In the planar case, the pressure p_p and fluid velocity u_p at the piston surface are the same as those just behind the shock. However, in the cylindrical and spherical cases, the flow field between the shock and the piston surface is nonuniform and can be obtained by using a similarity solution procedure [1].

In order to determine the power-energy relation using Eqs.(3,4), we also need to know t_{cr}. Previously we set this time equal to the induction delay time corresponding to the conditions at the piston surface. In this paper we critically look at this assumption by comparing the results from the above theoretical model to those from detailed numerical simulations. The numerical model used for these detailed simulations is briefly described below.

The Numerical Model

The one-dimensional reactive shock model [6,7] used to perform the simulations solves the time-dependent conservation equations for mass, momentum and energy coupled to the equations describing the chemical kinetics. The model uses an explicit, Eulerian finite difference formulation with a sliding rezone capability to provide resolution around moving gradients. The solutions of the equations describing the fluid dynamics and the chemistry of the problem are coupled using time-step splitting techniques [7].

The convective transport terms in the conservation equations are solved using one variant of the Flux-Corrected Transport (FCT) method [8]. This is a conservative, monotonic algorithm with fourth-order phase accuracy and does not require artificial viscosity to stabilize shocks. The ordinary differential equations describing the chemical kinetics are solved using VSAIM, a vectorized version of the selected asymptotic integration method employed in CHEMEQ [9]. The chemical kinetics rate scheme consists of about fifty rates relating the species H_2, O_2, H, O, OH, HO_2, H_2O and H_2O_2.

Results and Discussion

We first used the theoretical model to determine the power-energy relations for the initiation of planar detonations in a hydrogen-oxygen-nitrogen (2:1:4) mixture. The initial temperature and pressure of the mixture were 298 K and 0.5 atm, respectively. The time duration necessary for successful initiation was assumed to be equal to the chemical induction time of the mixture corresponding to the conditions at the piston surface. The induction time used was obtained by integrating the same chemical kinetics rate equations used in the detailed simulations.

We then set up the numerical model described above to simulate shock tube experiments and this describes the same problem solved by the theoretical model. By varying the pressure ratio across the diaphragm of a uniform shock tube we obtained constant velocity shocks of various strengths in the driven section. The driven section was assumed to be filled with a hydogen-oxygen-nitrogen mixture (2:1:4) at 298 K and 0.5 atm to correspond to the conditions in the theoretical model. For each pressure ratio, we noted the times at which ignition and detonation occurred as well as the pressure and velocity at the contact surface. From these quantities we obtained the power and energy required to initiate a detonation.

The results from the detailed simulations agreed with the predictions of the theoretical model when the Mach number of the shock wave was high. However for low mach numbers, the detailed simulations showed initiation with lower energies than those predicted by the theoretical model. A closer look at the results showed that the pressures and temperatures near the contact surface were in the weak-ignition regime and therefore very sensitive to perturbations [10].

In order to evaluate quantitatively how a specific type of perturbation affects ignition, we then simulated the effects of sound waves in a hydrogen-oxygen-nitrogen mixture by reconfiguring the numerical model described earlier. This gave us a quantitative relation between the induction time and sound waves of various amplitudes and frequencies. The effect of such sound wave perturbations on the power-energy relation has also been determined.

Conclusions

From the results presented in this paper, we observe that:
(1) for the initiation of planar detonations, the appropriate time to use in the theoretical model is the induction time, provided the mixture under consideration is not sensitive to perturbations;
(2) for mixtures which are sensitive to perturbations, the power-energy relation will also depend upon the actual perturbations present in the system;
(3) the effect of sound wave perturbations of a range of amplitudes and frequencies on the power-energy relation has been determined.

Acknowledgements

The authors greatfully acknowledge the editorial assistance of Ms. D. Miller. This work has been supported by the Office of Naval Research through the Naval Research Laboratory.

References

1. Kailasanath, K. and Oran, E.S., The Relation between Power and Energy in the Shock Initiation of Detonations-I. Basic Theoretical Considerations and the Effect of Geometry. NRL Memorandum Report, Naval Research Laboratory, Washington, DC (to be published, 1983).

2. Kailasanath, K. and Oran, E.S., Power-Energy Relations for the Direct Initiation of Gaseous Detonations. Presented at the Ninth International Colloquium on the Dynamics of Explosions and Reactive Systems, Poitiers, France (1983).

3. Abouseif, G.E. and Toong, T.Y., Combust. Flame, 45, 39 (1982).

4. Taylor, G.I., Proc.Roy.Soc.(London), A 186, 273 (1946).

5. Chu, B.T., Pressure Waves Generated by Addition of Heat in a Gaseous Medium. NACA TN 3411, NACA, Washington, DC (1955).

6. Oran, E.S., Young, T.R., and Boris, J.P., Seventeenth Symposium (International) on Combustion, The Combustion Institute, Pittsburgh, PA, p. 43 (1979).

7. Oran, E.S., and Boris, J.P., Prog. Energy. Combust. Sci. 7, 1 (1981).

8. Boris, J.P. and Book, D.L., Methods of Computational Physics, Academic Press, New York, 1976, Vol.16, p.85.

9. Young, T.R., CHEMEQ,A Subroutine for Solving Stiff Ordinary Differential Equations. NRL Memorandum Report 4091, Naval Research Laboratory, Washington, DC (1980).

10. Oran, E.S. and Boris, J.P., Combust.Flame., 48, 149 (1982).

APPENDIX E

THE RELATION BETWEEN POWER AND ENERGY IN THE SHOCK INITIATION OF DETONATIONS - I. BASIC THEORETICAL CONSIDERATIONS AND THE EFFECTS OF GEOMETRY

NRL Memorandum Report 5179

The Relation Between Power and Energy in the Shock Initiation of Detonations

I. Basic Theoretical Considerations and the Effects of Geometry

K. KAILASANATH* AND E. S. ORAN

Laboratory for Computational Physics

**Science Applications Inc.*
McLean, VA 22102

September 15, 1983

This work was supported by the Office of Naval Research.

NAVAL RESEARCH LABORATORY
Washington, D.C.

SECURITY CLASSIFICATION OF THIS PAGE (When Data Entered)

REPORT DOCUMENTATION PAGE	READ INSTRUCTIONS BEFORE COMPLETING FORM
1 REPORT NUMBER: NRL Memorandum Report 5179	2 GOVT ACCESSION NO. 3 RECIPIENT'S CATALOG NUMBER
4 TITLE (and Subtitle): THE RELATION BETWEEN POWER AND ENERGY IN THE SHOCK INITIATION OF DETONATIONS I. Basic Theoretical Considerations and the Effects of Geometry	5 TYPE OF REPORT & PERIOD COVERED: Interim report on a continuing NRL problem. 6 PERFORMING ORG. REPORT NUMBER
7 AUTHOR(s): K. Kailasanath* and E.S. Oran	8 CONTRACT OR GRANT NUMBER(s)
9 PERFORMING ORGANIZATION NAME AND ADDRESS: Naval Research Laboratory Washington, DC 20375	10 PROGRAM ELEMENT, PROJECT, TASK AREA & WORK UNIT NUMBERS: 44-1950-0-3
11 CONTROLLING OFFICE NAME AND ADDRESS	12 REPORT DATE: September 15, 1983 13 NUMBER OF PAGES: 45
14 MONITORING AGENCY NAME & ADDRESS(if different from Controlling Office)	15 SECURITY CLASS (of this report): UNCLASSIFIED 15a DECLASSIFICATION/DOWNGRADING SCHEDULE
16 DISTRIBUTION STATEMENT (of this Report): Approved for public release; distribution unlimited.	
17 DISTRIBUTION STATEMENT (of the abstract entered in Block 20, if different from Report)	
18 SUPPLEMENTARY NOTES: *Present address: Science Applications Inc., McLean, VA 22102 This work was supported by the Office of Naval Research.	
19 KEY WORDS (Continue on reverse side if necessary and identify by block number): Detonation; Minimum detonation energy; Acetylene-oxygen mixtures; Detonation initiation	

20 ABSTRACT (Continue on reverse side if necessary and identify by block number)

Recent studies on the direct initiation of gaseous detonations have shown that initiation depends not only on the energy deposited but also on the rate at which it is deposited, namely the power. In this paper, we have used a theoretical model to determine the relation between the power and the energy required for the initiation of planar, cylindrical and spherical detonations in a detonable gas mixture. The results from the model show that the qualitative differences in the power-energy

(Continues)

DD FORM 1 JAN 73 1473 EDITION OF 1 NOV 65 IS OBSOLETE
S/N 0102-014-6601

SECURITY CLASSIFICATION OF THIS PAGE (When Data Entered)

20. ABSTRACT (Continued)

relations obtained from two different experimental arrangements are due to differences in the geometry. We also show that the minimum power requirement corresponds to a shock of minimum Mach number only in the case of planar detonations. Finally, the effect on the power-energy relation of the ratio of specific heats and the experimental uncertainties in the determination of the induction times have been studied for an acetylene-oxygen-nitrogen mixture.

CONTENTS

THE RELATION BETWEEN POWER AND ENERGY IN THE SHOCK INITIATION OF DETONATIONS

I. Basic Theoretical Considerations and the Effects of Geometry

I. INTRODUCTION

The early studies of direct initiation of gaseous detonations[1,2,3] established the importance of the magnitude of the source energy. More recent experiments[4,5,6] have shown the importance not only of the energy but also of the rate at which the energy is deposited, namely the power. The experimental results of Lee et al.[5] indicate that there is a minimum detonation energy, E_m, below which a detonation would not occur no matter what the power is and that there is a minimum power, P_m, below which a detonation would not occur no matter what the total energy is. Later, they noted[6] that the requirement for a minimum value for the power of the source indicates that the source must be capable of generating a shock wave of certain minimum strength (Mach number). They also concluded that the minimum energy requirement implied that the shock wave must be maintained at or above this minimum strength for a certain minimum duration.

Recently these ideas have been used by Dabora[7,8] to obtain a relation between the power and energy required for the direct initiation of hydrogen-air detonations in a shock tube. However, this power-energy relation is very different qualitatively from those of Knystautas and Lee[6]. More recently Abouseif and Toong[9] have proposed a simple theoretical model to determine the power-energy relation and predict their respective threshold values. The predictions based on their model were in qualitative agreement with the experiments of Knystautas and Lee[6].

Manuscript approved June 22, 1983.

In this paper we have modified and extended the basic model proposed by Abouseif and Toong[9] and have used it to determine the relation between the power and the energy required for the initiation of planar, cylindrical and spherical detonations in a detonable gas mixture. Specifically, we discuss its application to a stoichiometric oxy-acetylene mixture. We have used the results from the model to explain the qualitative differences between the experimental results of Knystautas and Lee[6] and Dabora[7]. The relation between the minimum power requirement and the Mach number of the shock wave has also been examined. Some of the limitations of the model are discussed, and several applications are described.

II. THE THEORETICAL MODEL

We can, in principle, study the direct initiation of detonations by performing detailed numerical simulations of the flow field generated by a given source of energy. In general, such a calculation is a complicated, multidimensional, multispecies, time-dependent problem. Part of the complication and cost of such calculations arises from the solution of the conservation equations, and part of it arises from integrating the large number of ordinary differential equations describing the chemical reactions. This latter factor is further complicated by the fact that we usually do not have an adequate representation of the chemical reactions with which to work. Thus, a convenient, inexpensive way to evaluate the relative tendency of different explosive mixtures to detonate would be very useful. Below we develop and expand a simple theoretical model proposed earlier by Abouseif and Toong[9]. Although this approach is not as precise as solving the full set of equations numerically, it offers a number of important insights and gets around the requirement of knowing the detailed chemical kinetics.

The model considers the flow generated by the motion of a constant velocity shock wave in planar, cylindrical and spherical geometries. As this shock wave passes through a gas mixture, the gas temperature and pressure increases. Due to this increase in temperature and pressure, ignition can occur in the shock heated gas mixture after the elapse of a certain time and this may lead to a detonation.

A constant velocity shock wave can be formed in each of the three geometries by the motion of a constant velocity piston[10,11]. Furthermore, it has been shown[11] that a pressure and velocity field identical to that ahead of a constant velocity piston can be generated by appropriate energy

addition. In Appendix A we have derived expressions for the energy and the power which must be delivered by a source to generate a constant velocity piston in the three geometries. The source power required is given by

$$P_s(t) = \frac{\gamma}{(\gamma-1)} C_\alpha p_p u_p^\alpha t^{\alpha-1} \quad , \qquad (1)$$

where $C_\alpha = 1, 2\pi, 4\pi$ for $\alpha = 1,2,3$ corresponding to the planar, cylindrical and spherical geometries respectively; p_p and u_p are the pressure and velocity at the piston surface and t is the duration of energy deposition. The energy deposited is given by the time integral of the power, that is

$$E_s(t) = \frac{\gamma}{(\gamma-1)} \frac{C_\alpha}{\alpha} p_p u_p^\alpha t^\alpha \quad . \qquad (2)$$

From the above equations we note that a planar energy source with a constant rate of energy deposition can generate a constant velocity piston in a planar geometry. An example of such an energy source is the high pressure driver in a uniform shock tube. However for a constant velocity piston in a cylindrical geometry, we need a line source with a rate of energy deposition proportional to time, and in a spherical geometry we need a point source with an energy deposition rate proportional to the second power of the time.

Equations (1) and (2) give the source power and the source energy required to generate a constant velocity piston in the three geometries. As shown later (in Appendix B), if the piston velocity is steady, a constant velocity shock wave could be generated ahead of it. If the piston velocity is reduced (by altering the energy deposition rate), rarefaction waves will be generated ahead of it and these, on catching up with the shock wave , will

reduce the shock velocity. However if the shock has been in motion for a sufficiently long time, chemical reactions would begin in the shock heated gas mixture. Then, even if the piston decelerates and produces rarefaction waves, these will have very little effect on the motion of the shock. In this case we could have a detonation.

Let us call the minimum time of shock travel required to initiate a detonation t_{cr}. Using this in Eqs. (1) and (2), we have

$$(E_s)_{cr} = \frac{\gamma}{(\gamma-1)} \frac{C_\alpha}{\alpha} p_p u_p^\alpha t_{cr}^\alpha \quad . \tag{3}$$

and

$$(P_s)_{cr} = \frac{\gamma}{(\gamma-1)} C_\alpha p_p u_p^\alpha t_{cr}^{\alpha-1} \quad . \tag{4}$$

In the planar case, the pressure p_p and fluid velocity u_p at the piston surface are the same as those just behind the shock. However, in the cylindrical and spherical cases, the flow field between the shock and the piston surface is nonuniform and can be obtained by solving the governing partial differential equations. However, the solution procedure is considerably simplified if we seek a similarity solution. The details of this solution procedure are given in Appendix B.

In order to determine the power-energy relation using Eqs. (3,4) we also need to know t_{cr}. This time must at least be equal to the time at which ignition first occurs in the flow field[9]. As noted by Urtiew and Oppenheim,[12] ignition usually occurs first at the contact surface (i.e., at the piston surface here) since the temperature and pressure is highest at this location. So a first estimate of the time t_{cr} would be the induction delay time corresponding to the conditions at the piston surface.

III. RESULTS AND DISCUSSION

We have used the model described above to determine the power-energy relations for the initiation of planar, cylindrical, and spherical detonations in a stoichiometric oxy-acetylene mixture. The initial temperature and pressure of the mixture were taken to be 300 K and 100 torr (0.1316 atm) to correspond to the initial conditions in the experiments of Knystautas and Lee[6]. As a first approximation, the time duration necessary for successful initiation was assumed to be equal to the chemical induction time of the mixture corresponding to the conditions at the piston surface.

The critical source power given by Eq. (4) is time dependent for the cylindrical and spherical cases. In order to relate the critical source energy to a critical source power, we need to define an average or "effective" power. Following Abouseif and Toong[9], we define an average critical source power as

$$(P_s)_{av} = \frac{(E_s)_{cr}}{t_{cr}}. \qquad (5)$$

This power also corresponds to the critical peak averaged power of the source as defined by Knystautas and Lee[6]. For the discussion below, we have used the terms power and energy to refer to the average critical source power (Eq. (5)) and the critical source energy (Eq. (3)).

A. Cylindrical Detonations in an Acetylene-Oxygen-Nitrogen Mixture

We have determined the power-energy relation for the initiation of cylindrical detonations using Eqs. (3) and (5). The induction time data used were those obtained by Edwards et al.[13] for an acetylene-oxygen-nitrogen (2:5:4) mixture and are given by:

$$\text{Log}\,(\tau[O_2]) = -9.41\ (\pm\ 0.2) + \frac{71.35\ (\pm\ 3.34)}{19.14\ T} \qquad (6)$$

where τ is the induction time in seconds, $[O_2]$ is the concentration in mol/liter, and T is the temperature in thousands of degrees K. Three different power-energy relations obtained from the theoretical model are shown in Figure 1. Curve A was obtained by using the smallest value of the induction time given by Eq. (6), that is, by choosing the negative signs. Curve B was obtained by using the mean values and curve C by using the largest value of the induction time (by choosing the positive signs). The arrows on curve C indicate the direction of increasing Mach number. First, we note that each curve has a minimum power and a minimum energy. We also observe that as the Mach number decreases below the Mach number corresponding to the minimum power, both the average source power and the source energy increase. However, when the Mach number increases above the Mach number corresponding to the minimum power, the energy first decreases to the minimum energy and then increases again. All three curves exhibit these same qualitative trends.

The shape of these curves can be explained in the following manner. As the Mach number of the shock wave decreases, the pressure and the temperature behind it decrease. This decrease also results in a decrease of the pressure and velocity at the piston surface. This would tend to decrease both the power and the energy since, as seen in Eqs. (1,2),

$$p \sim p_p u_p^2 t \tag{7}$$

$$E \sim p_p u_p^2 t^2 \quad . \tag{8}$$

This tendency is, however, opposed by the tendency of the induction time to increase with decreases in the pressure and the temperature. For low Mach numbers, (i e., low temperatures behind the shock) a small decrease in the Mach number of the shock wave leads to a large increase in the induction

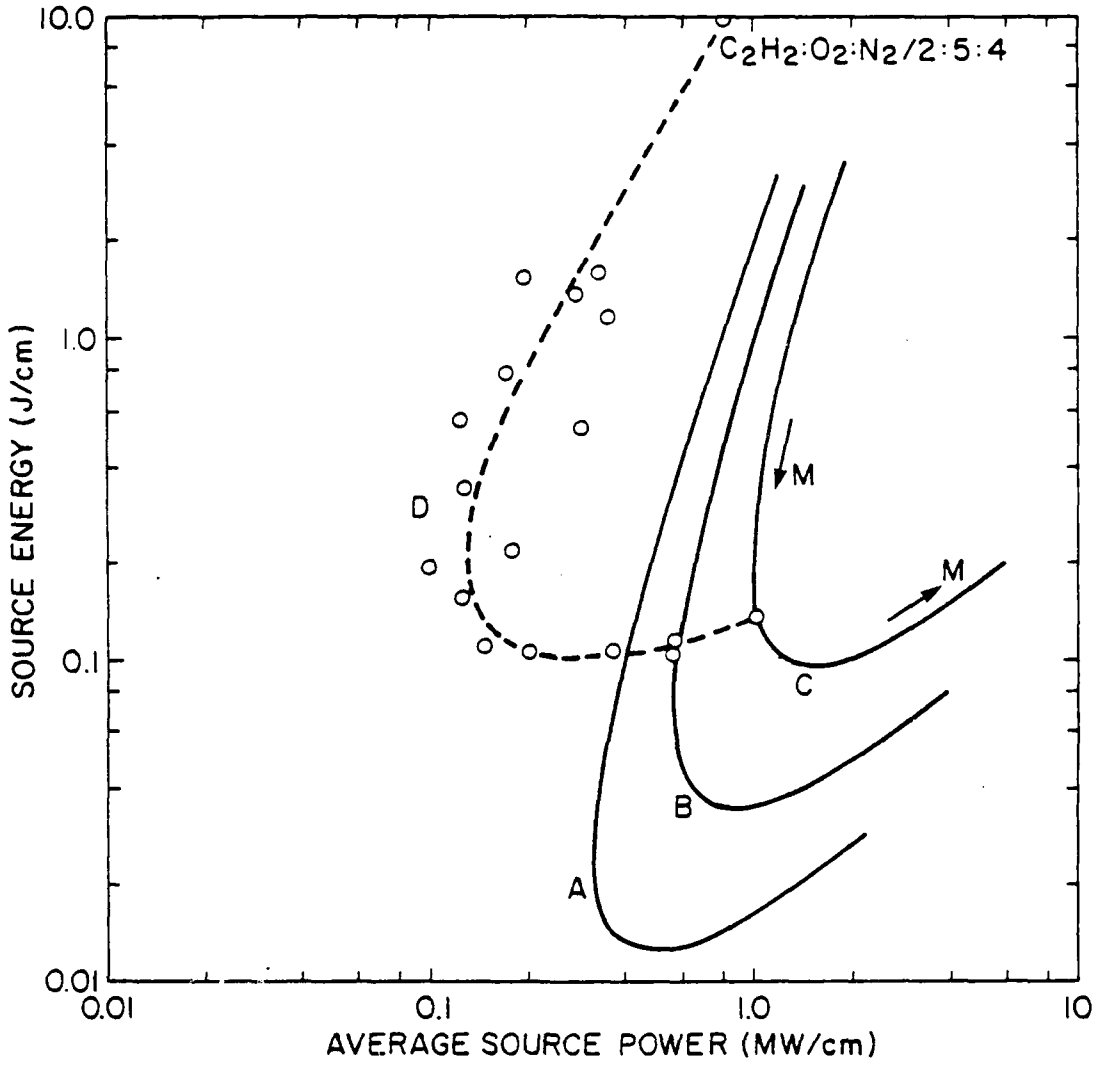

Figure 1. Power-energy relations for the initiation of cylindrical detonations in an acetylene-oxygen-nitrogen mixture (2:5:4) at 0.1316 atm and 300K. The data for curve D was obtained from spark ignition experiments [6]. Curves A, B, and C are explained in the text. The arrows on Curve C indicate the direction of increasing Mach number.

time. The shape of the curves in Figure 1 implies that this increase in induction time is more than sufficient to compensate for the decrease in the pressure and the velocity for Mach numbers below that corresponding to the minimum power. Therefore both the power and the energy increase with decreasing Mach number. Since the energy is proportional to the product of the power and the induction time (Eqs. (7,8)), the energy increases faster with induction time than the power does. As the Mach number increases above that corresponding to the minimum power, the increase in the pressure and velocity is larger than the decrease in the induction time. Therefore the power increases. However, for a certin range of Mach numbers, the increase in the pressure and velocity is not sufficient to compensate for the decrease in the square of the induction time. Therefore the energy decreases until it attains a minimum value, even though the power increases. Finally, for Mach numbers above that corresponding to the minimum energy, the increase in the pressure and velocity are easily able to overcome the decrease in the induction time with increasing Mach number and both the power and the energy increase. This occurs because the rate of decrease of the induction time with temperature is small for high temperatures (i.e., high Mach numbers) according to Eq. (6).

The power-energy curve obtained using data from the spark ignition experiments[6] of Knystautas and Lee has also been included in Figure 1 as curve D. The data for curve D is the same as that used by Abouseif and Toong[9] for their Figure [1], and was originally presented in Figure [4] of Knystautas and Lee[6]. Curve D exhibits the same qualitative trends as those of the theoretical curves discussed above. However, we observe that the values of the minimum power and the minimum energy from the four curves are

very different from each other. The differences in the values of these parameters from the three "theoretical" curves (A,B, and C) indicate that the experimental uncertainties in the values of the induction times used have a significant effect on the value of the minimum power and the minimum energy. The minimum power varies from about 0.3 MW/cm to about 1 MW/cm and the minimum energy varies from about 0.012 J/cm to about 0.1 J/cm. The experimentally determined minimum power (from curve D) is about 0.13 MW/cm, which is lower than the calculated values, and the minimum energy is about 0.1 J/cm, which is at the top of the range of calculated values.

The quantitative differences between the experimental and theoretical values could be due to a variety of factors, a few of which we now discuss. As observed from curves A, B, and C, uncertainties in the induction time data can have a significant effect on the values of the minimum power and the minimum energy. Expressions such as Eq. (6) for the induction time are obtained by fitting to a limited range of experimental data. However, here we have used Eq. (6) for a range of temperatures and pressures far greater than that over which it was determined. The Mach numbers and the corresponding temperatures and pressures at the shock and the piston surface, along with the induction time used for obtaining curve B, are given in Table I. We see that for Mach numbers greater than about 14, the temperatures and pressures are so high that the entrapolated induction time is of questionable validity. However, for obtaining the theoretical results, we had assumed a constant value of 1.2 for γ, the ratio of specific heats. We see from Table I that for high Mach numbers, the γ of the shocked gas could be very different from that ahead of the shock wave because of the large temperature differences. Using an incorrect value for γ could also

AD-A142 402 ENERGY RELEASE AND FLUID DYNAMICS IN MULTIPHASE SYSTEMS (U) SCIENCE APPLICATIONS INC MCLEAN VA K KAILASANATH 18 APR 84 SAI-84/1093 N00014-82-C-2037 2/2

UNCLASSIFIED F/G 20/4 NL

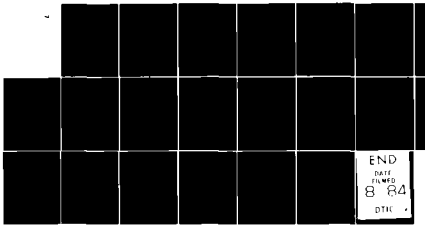

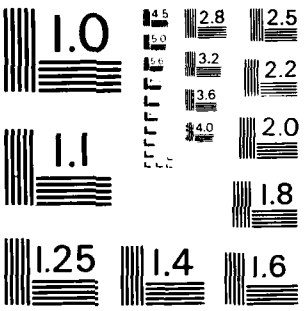

MICROCOPY RESOLUTION TEST CHART

NATIONAL BUREAU OF STANDARDS - 1963 - A

TABLE I

Parameters at the Piston Surface for Shocks of Different Strengths

M	P_s(atm)	T_s(K)	p_p(atm)	T_p(K)	τ_p(μsec)
4.0	2.285	769.5	2.378	774.6	1485.3
5.0	3.577	1037.9	3.701	1043.8	73.823
6.0	5.156	1365.4	5.320	1372.6	9.4207
7.0	7.023	1752.4	7.232	1761.0	2.2381
8.0	9.176	2198.8	9.439	2209.2	0.8003
9.0	11.616	2704.6	11.939	2717.0	0.37639
10.0	14.344	3270.0	14.736	3284.7	0.21357
12.0	20.661	4579.2	21.209	4599.2	0.098452
14.0	28.126	6126.3	28.859	6152.6	0.060420
16.0	36.740	7911.5	37.685	7945.0	0.043616
18.0	46.502	9934.6	47.687	9976.4	0.034733
20.0	57.413	12195.8	58.870	12246.8	0.029447

Note: A constant γ of 1.2 has been assumed for obtaining the above results.

explain some of the quantitative differences between the experimental and theoretical results.

B. Effect of γ on Power-Energy Relations

We have repeated the power-energy calculations using different but constant values for γ on both sides of the shock wave and the results are shown in Figure 2. We observe that γ does indeed have a significant effect on the minimum power and the minimum energy. When γ is changed from 1.1 to 1.4, the minimum source power decreases from 2.0 MW/cm to 0.18 MW/cm and the minimum energy decreases from 0.065 to about 0.02 J/cm. The Mach number at which the shock must travel to attain the minimum power is also very different, as seen in Figure 3 where the average source power is shown as a function of Mach number for three values of γ. Changing γ from 1.4 to 1.1 doubles the Mach number corresponding to the minimum power from 8 to 16. The effect of γ on the power-energy relation arises partly from the factor $(\gamma/\gamma-1)$ in Eqs. (3) and (4) and partly from the fact that the temperature behind a shock of given Mach number is very different for different γ's.

The effect of the factor $(\gamma/\gamma-1)$ is to change quantitatively the values of the source power and the source energy corresponding to the shock of a given Mach number and is the same for all Mach numbers. The changes in the temperature behind a shock wave due to assumed differences in γ is, however, a function of the shock Mach number. Let us consider a shock wave of the Mach number 10. In Table II we have given the pressure ratio, the temperature ratio and the temperatures across this shock wave for different values of γ. We have also included the case where γ is different across the shock wave as case 3. For obtaining case 3, Eqs. (C7-C13) from Appendix C

TABLE II

Effect of the Ratio of Specific Heats

CASE	γ_o	γ_s	p_s/p_o	T_s/T_o	T_o	T_s
1	1.2	1.2	109.000	10.900	300	3270.0
2	1.3	1.3	112.913	15.710	300	4712.89
3	1.3	1.2	118.426	11.454	300	3436.26

Note: The conditions ahead of the shock wave are denoted by "o" and those behind by "s".

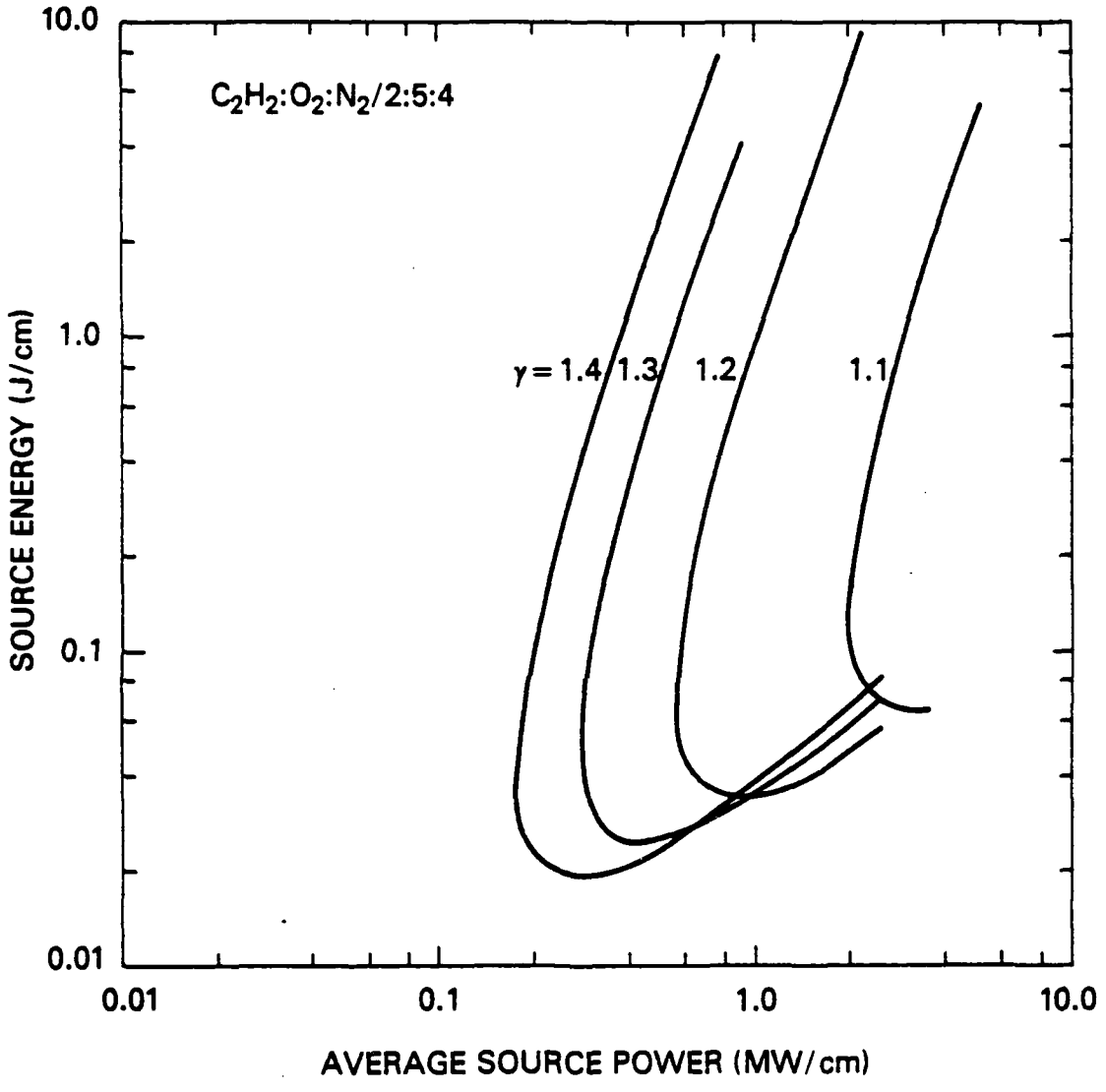

Figure 2. Effect of γ on the power-energy relations for the initiation of cylindrical detonations in an acetylene-oxygen-nitrogen mixture.

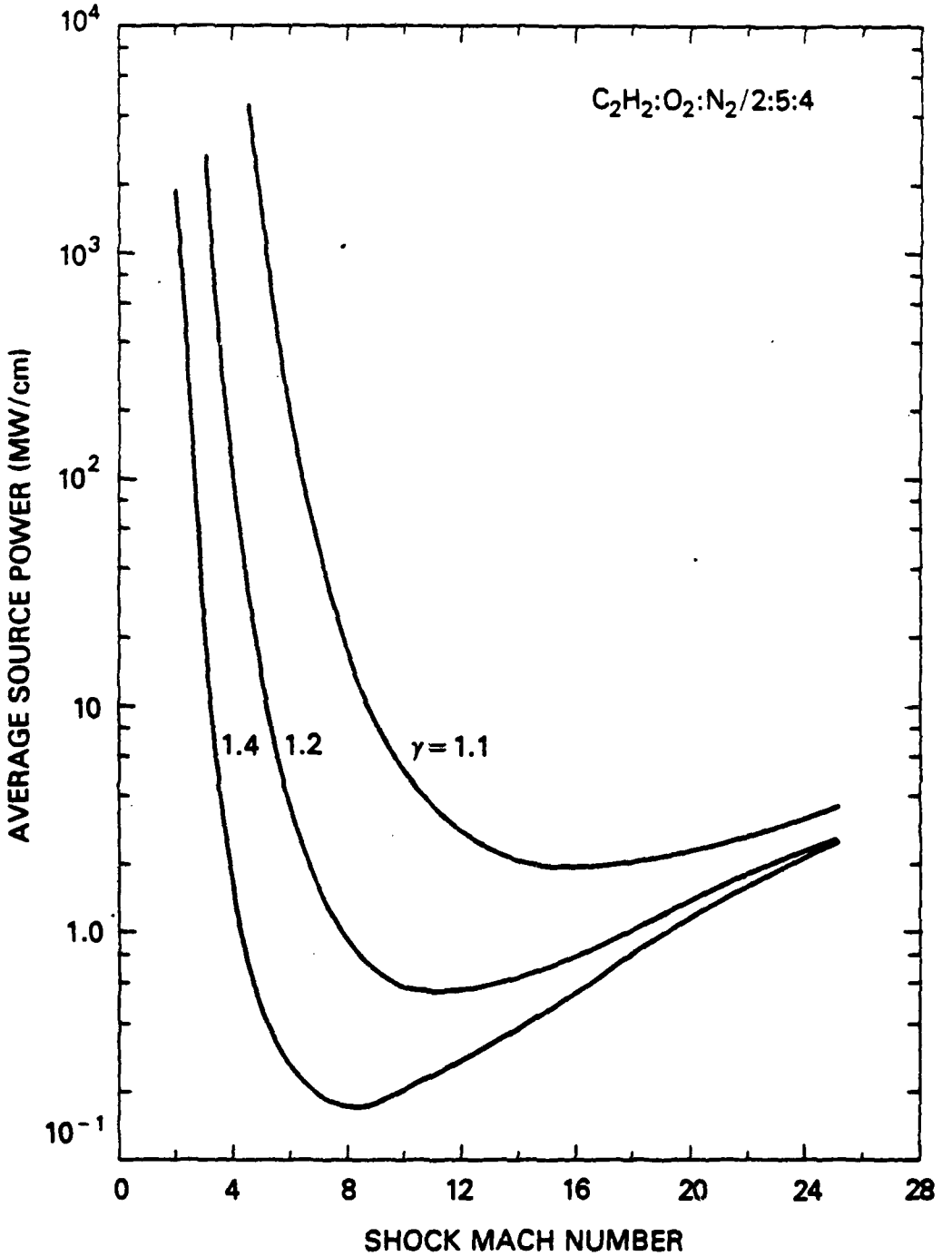

Figure 3. The average source power as a function of the shock Mach number for constant γ's across the shock wave.

were used. We see that the temperature behind the shock wave is significantly lower than that for case 2. Case 3 is a more realistic case than case 2, since γ is generally lower behind the shock. However, the appropriate γ for conditions behind the shock wave is different for different Mach numbers, since the temperatures are different. Thus a better approach is first to guess a γ for each Mach number and use it to calculate the temperature behind the shock. This new temperature implies a new γ, as discussed in Appendix C. Using this new γ in the modified shock relations (Eqs. (C7-C13)), we get a new temperature. This iterative procedure can be continued till convergence is achieved.

The power-energy calculations were repeated using the correct value for γ, that is, for each Mach number including the effect of temperature on γ. In Figures 4 and 5, the average source power and the source energy have been shown as functions of the Mach number for three different conditions (A, B, and C). Curves A and C were obtained assuming γ constant and have already been discussed. Curve B is obtained using the variable γ. For low Mach numbers, curve B lies close to curve A and for very high Mach numbers it tends towards curve C. This is not surprising since for the acetylene-oxygen-nitrogen mixture being studied here, γ varies from 1.31 to 1.16 when the Mach number changes from 2 to 24. From curve B in Figures 4 and 5 we also note that the minimum power and the minimum energy conditions occur at Mach number of 10.0 and 15.5 respectively. The power-energy curve obtained with the variable γ is shown as curve B in Figure 6 where we have also shown three other curves obtained assuming constant γ. We note that curve B lies predominantly between the curves with γ of 1.1 and 1.3 and is very similar to the curve with γ of 1.2.

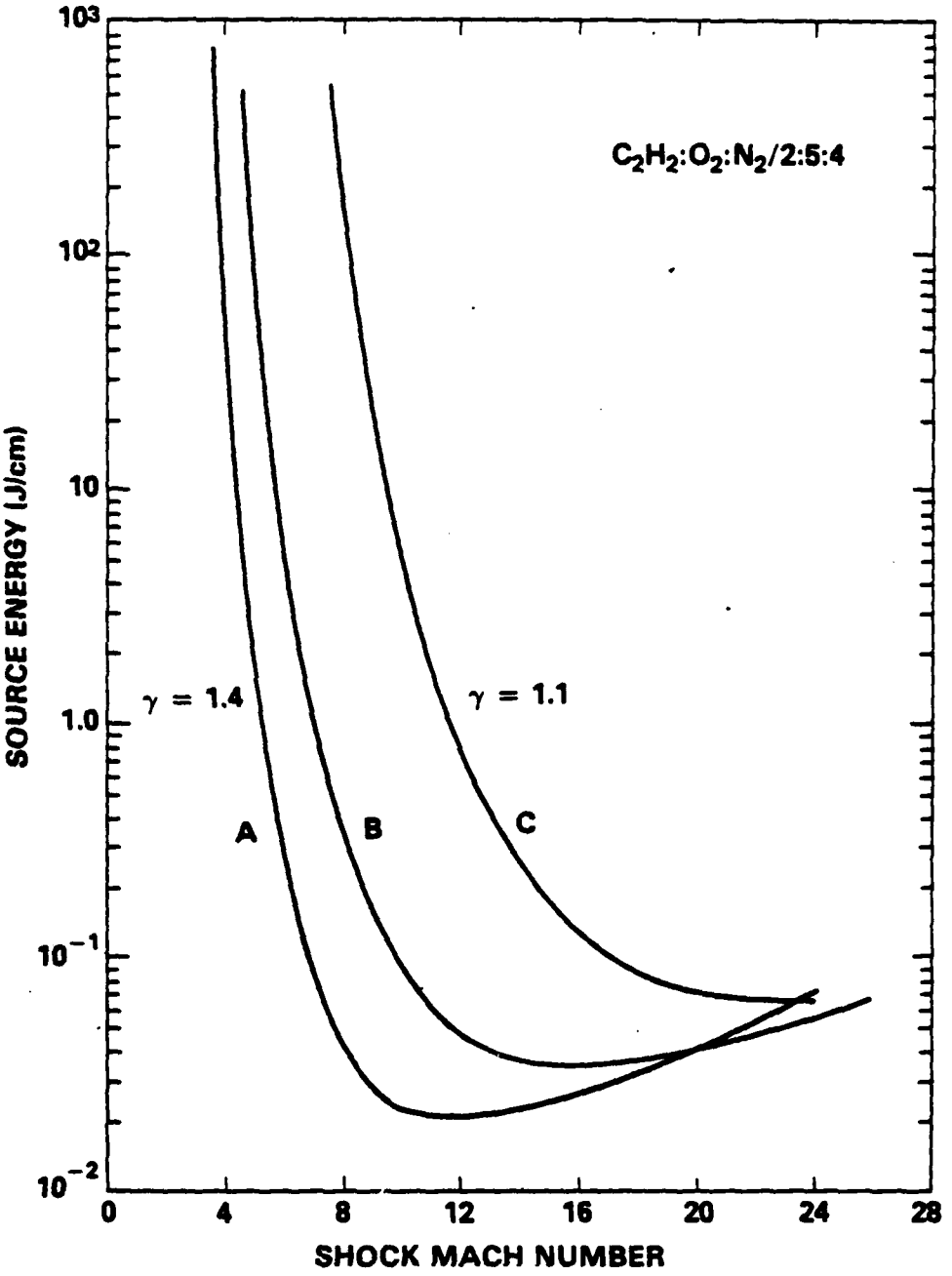

Figure 4. The source energy as a function of the shock Mach number. Curves A and C were obtained assuming γ to be constant across the shock wave. Curve B was obtained assuming γ to be variable as explained in the text.

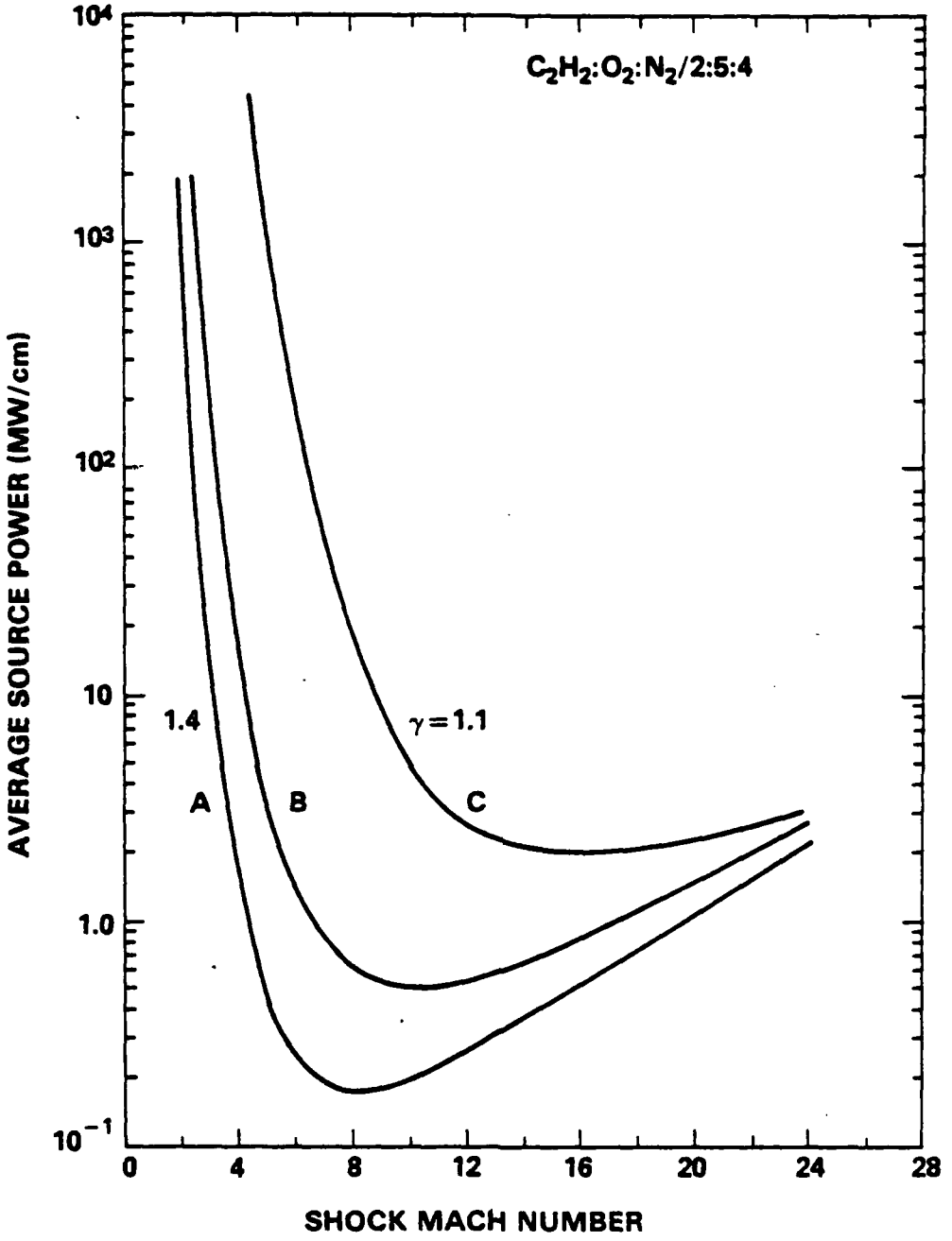

Figure 5. The average source power as a function of the shock Mach number. Curves A and C were obtained assuming γ to be constant across the shock wave. Curve B was obtained assuming γ to be variable as explained in the text.

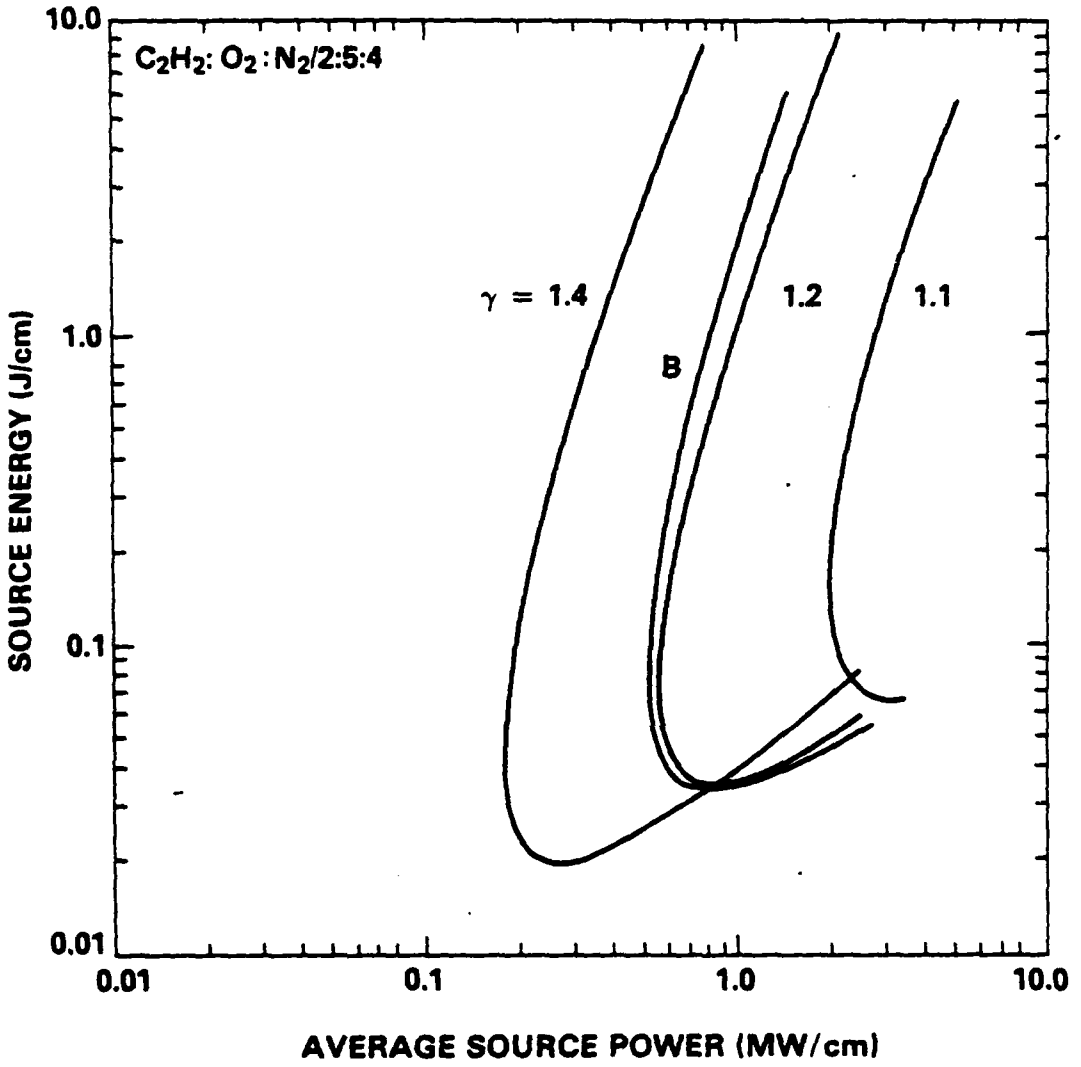

Figure 6. Effect of variable γ on the power-energy relations for the initiation of cylindrical detonations in an acetylene-oxygen-nitrogen mixture.

From the above discussion it is clear that the effect of using the correct γ is mainly to alter the Mach number corresponding to the minimum power and the minimum energy condition. However, the calculated values of the minimum power and the minimum energy are still different from those obtained experimentally. Therefore we examine another possible reason for the differences between the experimental and the theoretical values: the uncertainty in the appropriate time to be used for t_{cr} in Eqs. (3) and (5).

C. Critical Time for Energy Deposition

As a first approximation, we assume that energy must be deposited until ignition occurs at some point in the flow field between the shock and the piston surface. Since, in general, the temperature and pressure is highest at the piston surface, we used the chemical induction time corresponding to these conditions as the appropriate time for energy deposition. However, when there is fluid motion, ignition can occur before the time corresponding to the constant volume, homogeneous chemical induction time. For example, for a certain range of temperatures and pressures, oxy-hydrogen mixtures with small perturbations could have significantly reduced ignition times. The specific effect of this phenomenon on the power-energy relations will be reported in a subsequent paper. In gas mixtures which are not particularly sensitive to perturbations, the shortest induction time in the shocked region seems to be the necessary condition for the initiation of detonations. However, we need to consider whether this is a sufficient condition also.

Shock tube simulations[14] have indicated that the time at which a detonation wave is first observed is only very slightly longer than the time at which ignition first occurs. That is, the time between ignition and the

formation of a detonation wave is small when compared to the induction time. This is not surprising when we consider the fact that for many reactive systems, the reaction time is very small compared to the induction time. The results of Abouseif and Toong on the initiation of planar detonations[9] also supports this observation. However we have not studied the effect of geometry on the time between ignition and detonation. It could very well be that due to the volume change in spherical and cylindrical geometries, this time is significant when compared to the induction time. This needs to be studied before one can confidently use the induction time as the appropriate time for t_{cr}.

We have compared the results from the theoretical model for the case of cylindrical detonations with the experimental results of Knystautas and Lee[6] because in both cases the amount of energy deposited was proportional to the second power of the time. However, it is important to note that in the theoretical model we have considered only constant velocity shock waves and it was this that made it possible to assign a single induction time to each shock wave. If the velocity of the shock wave is not constant, it is not possible to assign a single induction time to it since the flow field behind the shock wave would be time-dependent. Thus, shock waves of different time histories can deposit the same amount of energy but at different average source powers. This could be an imporant factor in the quantative differences between the experimental and theoretical values.

D. Initiation of Planar Detonations

The derived power-energy relation for the initiation of planar detonations in the same oxy-acetylene mixture is shown in Figure 7. In this

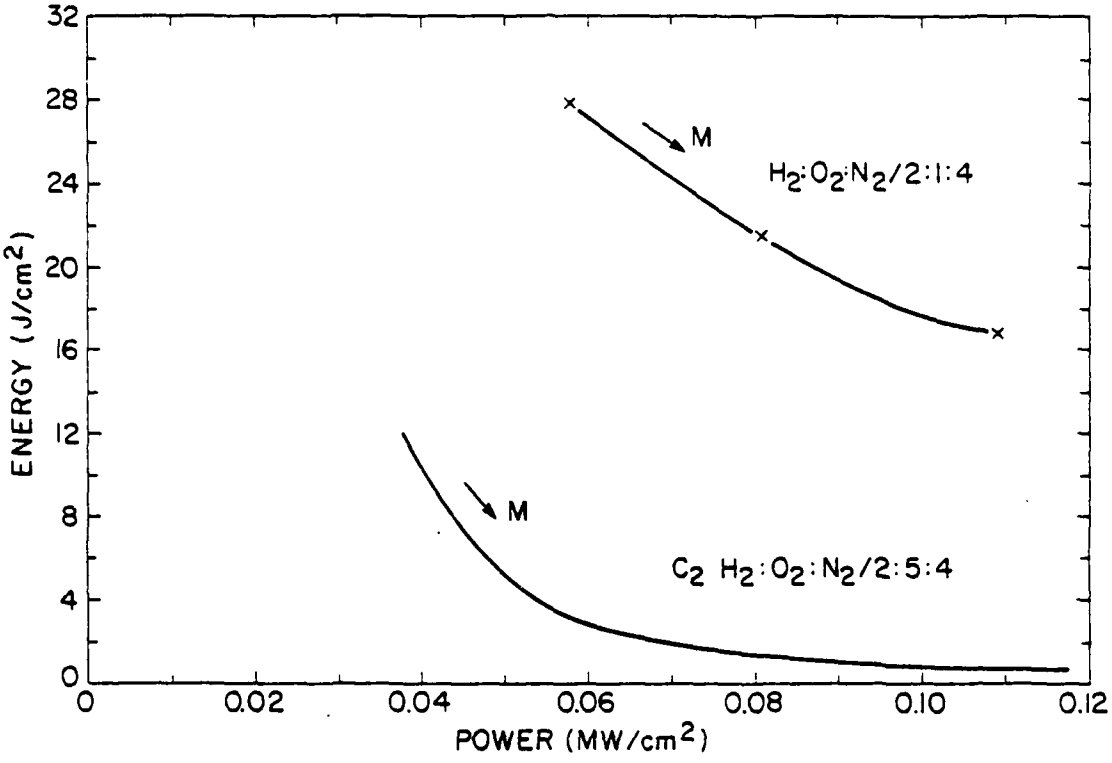

Figure 7. Power-energy relations for the initiation of planar detonations. The x's are data obtained from shock tube experiments [7].

figure, we also show the shock tube data of Dabora[7] on the direct initiation of detonations in a stoichiometric hydrogen-air mixture. The point to notice is that both curves exhibit the same qualitative behavior. Unlike the cylindrical case, each value of the power corresponds to an unique value of energy. The direction of increasing shock strength (as determined by the Mach number) is also shown in Figure 7. In the planar case, we see that as the Mach number decreases the power always decreases. As noted earlier in the cylindrical case, as the Mach number decreases, the power decreases only up to the minimum power. Then the power increases with a decrease in the Mach number of the shock wave. Therefore, the qualitative difference in the experimental data of Knystautas and Lee (shown in Figure 1) and Dabora (shown in Figure 7) are due to the difference in the geometry of the two experiments.

We also observe in Figure 7 that as the Mach number decreases, we need more and more energy to initiate a detonation. The trend of the curves indicates that there is a minimum Mach number below which a detonation will not occur (i.e., would require an infinite amount of energy). The value of the power corresponding to this minimum Mach number is the minimum power. This agrees with the observation made by Knystautas and Lee[6] that the requirement for a minimum value of the source power indicates that the source must be capable of generating a shock wave of a certain minimum Mach number. However, we observe from Figure 1 (see also Figures 3 and 5) that for the case of cylindrical detonations, the minimum power does not correspond to the shock wave of minimum Mach number. In the cylindrical case, it is possible to initiate a detonation with a shock wave of lower Mach number than that corresponding to the minimum power. Such a shock will have to be maintained

for a longer time than the shock corresponding to the minimum power and hence will require a larger amount of energy.

E. Initiation of Spherical Detonations

The power-energy curve for the initiation of spherical detonations is similar to the curve for the cylindrical case. However, for the case of spherical detonations, the power is

$$P \sim p_p u_p^3 t^2, \tag{9}$$

but the energy is still

$$E \sim P t. \tag{10}$$

Since the power and energy are proportional to higher powers of the time, t, uncertainties in t will have a greater effect on the value of the minimum power and the minimum energy. Further work is being carried out currently to study the initiation of spherical detonations in hydrogen-air mixtures and to compare this to experimental data.

IV. SUMMARY AND CONCLUSIONS

In this paper we have used a theoretical model to determine the relation between the power and the energy required for the initiation of planar, cylindrical and spherical detonations in a gas mixture. The results discussed above show that though the simple theoretical model has significant limitations, it can still be used to explain the qualitative differences in the power-energy relations obtained from different experimental arrangements. Another result from the model is that the minimum power requirement corresponds to a shock of minimum Mach number only in the case of planar detonations.

The results from the model on the initiation of cylindrical detonations in an acetylene-oxygen-nitrogen mixture qualitatively agrée with experimental data. Some of the reasons for the quantitative differences have been examined. One of the important parameters in the model is the time required for deposition of the critical energy required for the initiation of detonations. This time is related to the induction time and the results presented above show that uncertainties in the induction time data used can have a significant effect on the power-energy relations. The results also indicate that further work needs to be done to determine the effect of the geometry on the time for critical energy deposition.

The quantitative differences between the experimental and theoretical results may also arise because of the model assumption that the velocity of the shock wave is constant. This may not be so in the experiments. Furthermore, the model considers only the minimum power and energy required to initiate a detonation wave. We have not examined whether this would result in a self-sustained, propagating detonation wave. Detonation

propagation is characterized by complicated interactions among incident shock waves, transverse waves and Mach stems which form detonation cells. These must be described by multidimensional theories and simulations. The results from such studies need to be considered to extend the work presented here to the study of self-sustained detonation waves.

One application of the model presented here is to determine the relative tendency of different explosives to detonate, since the limitations of the model would then be less critical. This would be particularly useful for studying the effect of additives on the detonability of condensed phase explosives. Further work is being carried out to modify the model for such applications.

Appendix A

Source Power and Energy Required to Generate a Constant Velocity Piston

Here we derive the power and energy required by a source to generate a constant velocity piston in planar, cylindrical and spherical geometries. Let us first calculate the work done by a constant velocity piston moving from time t_o to time t in a gas mixture. If the effects of viscosity, heat conduction and chemical reaction are negligible during the time internal $(t-t_o)$, the pressure ahead of the constant velocity piston would also be constant. Then the work done by the piston on the gas mixture is given by

$$w = \int_{v_o}^{v} p_p \, dv = p_p \, (v - v_o) \qquad \text{(A1)}$$

where v_o and v are the volumes at time t_o and t, repectively. The volume change $(v - v_o)$ depends on the geometry of the system. In planar geometry, the volume swept out by the piston is

$$v - v_o = A(r-r_o) \quad , \qquad \text{(A2)}$$

where r_o is the position of the piston at time t_o and A is the cross sectional area of the planar piston. In cylindrical geometry,

$$v - v_o = \ell \, (\pi r^2 - \pi r_o^2) \quad , \qquad \text{(A3)}$$

where ℓ is the characteristic linear dimension of the system and in a spherical geometry,

$$v - v_o = \frac{4}{3} \pi r^3 - \frac{4}{3} \pi r_o^3 \quad . \qquad \text{(A4)}$$

The position of the constant velocity piston at time t is given by

$$r = r_o + u_p (t - t_o) \quad , \tag{A5}$$

where u_p is the velocity of the piston. Without loss of generality we can assume that $r_o = 0$ at time $t_o = 0$. Using Eq. (A5) in Eqs. (A2), (A3) and (A4), we have

$$v - v_o = \frac{B_\alpha}{\alpha} u_p^\alpha t^\alpha \quad , \tag{A6}$$

where $B_\alpha = A$, $2\pi\ell$, and 4π for α=1, 2, and 3 corresponding to the planar, cylindrical and spherical geometries respectively.

Substituting Eq. (A6) into Eq. (A1) we have

$$w = p_p \frac{B_\alpha}{\alpha} u_p^\alpha t^\alpha \quad . \tag{A7}$$

Defining

$$w_p = \frac{w}{A} \quad \text{for } \alpha = 1 \quad ,$$

$$= \frac{w}{\ell} \quad \text{for } \alpha = 2 \quad , \text{ and} \tag{A8}$$

$$= w \quad \text{for } \alpha = 3 \quad ,$$

we have

$$w_p = \frac{C_\alpha}{\alpha} p_p u_p^\alpha t^\alpha \quad . \tag{A9}$$

It is important to note that the above expression for w_p gives the work done by the piston, per unit area in planar geometry and per unit length in cylindrical geometry.

In order to obtain the above amount of work w_p, we will need a source which can generate and maintain such a constant velocity piston. It has been shown that a pressure and velocity field identical to that ahead of such a piston can be generated by appropriate heat addition. In order to demonstrate this, consider heat addition to a closed system of arbitrary volume v_o. For such a system with no heat losses to the surroundings, the first law of thermodynamics states that the change in the internal energy of the system is

$$dE_{int} = dq + dw \tag{A10}$$

where dq is the amount of heat energy deposited and dw is the work done by the system. Let us assume that heat energy is added to the system to take it from the volume v_o to the volume v at a constant pressure, p. Then, the change in the internal energy of the system (assuming a mixture of perfect gases) is given by

$$dE_{int} = \frac{pv}{\gamma-1} - \frac{pv_o}{\gamma-1} = \frac{p}{\gamma-1}(v-v_o). \tag{A11}$$

The work done by the system in going from v_o to v at the constant pressure p is

$$dw = -\int_{v_o}^{v} pdv = -p(v-v_o). \tag{A12}$$

Substituting Eqs. (A11) and (A12) in Eq. (A10), we find that the amount of heat energy which has to be deposited to create the required change in the system is

$$E_{dep} = \frac{p}{\gamma-1}(v-v_o) + p(v-v_o)$$

$$= \frac{\gamma}{\gamma-1} p (v-v_o)$$

$$= \left(\frac{\gamma}{\gamma-1}\right) w. \tag{A13}$$

Substituting Eq. (A9) in Eq. (A13) we have the source energy required to create a constant velocity piston in the three geometries,

$$E_s(t) = \frac{\gamma}{\gamma-1} \frac{C_\alpha}{\alpha} p_p \, u_p^\alpha + t^\alpha \quad . \tag{A14}$$

The power, or the rate at which energy is deposited, is given by

$$P_s(t) = \left.\frac{dE_s}{dt}\right|_t$$

$$= \frac{\gamma}{\gamma-1} C_\alpha \, p_p \, u_p^\alpha \, t^{\alpha-1}. \tag{A15}$$

Appendix B

Flow Field between the Piston Surface and Shock Wave

In the planar case, the pressure and fluid velocity at the piston surface are the same as those just behind the shock. However, in the cylindrical and spherical cases, the flow field between the shock and the piston surface is nonuniform but can be obtained by solving the following equations. For a one-dimensional flow, the equations for the conservation of mass can be written as:

$$\frac{\partial \rho}{\partial t} + u \frac{\partial \rho}{\partial r} + \rho \left[\frac{\partial u}{\partial r} + (\alpha-1) \frac{u}{r} \right] = 0, \tag{B1}$$

and for conservation of momentum as:

$$\frac{\partial u}{\partial t} + u \frac{\partial u}{\partial r} = - \frac{1}{\rho} \frac{\partial p}{\partial r} , \tag{B2}$$

where α = 1, 2, and 3 for planar, cylindrical and spherical coordinates respectively. Since we are primarily concerned with the flow field before any significant reactions occur, we can assume the flow is isentropic if diffusive transport effects are negligible. For a perfect gas, the energy equation then becomes

$$\frac{dp}{d\rho} = \frac{\gamma p}{\rho} . \tag{B3}$$

We can obtain the flow field between the piston surface and the shock wave by solving the above system of partial differential equations with appropriate boundary conditions. However, the solution procedure is considerably

simplified if we seek a similarity solution. Then the system of partial differential equations can be reduced to a system of coupled ordinary differential equations:

$$\frac{(u-L)}{\rho}\frac{d\rho}{dL} + \frac{du}{dL} + (\alpha-1)\frac{u}{L} = 0 \qquad \text{(B4)}$$

$$(u-L)\frac{du}{dL} = -\frac{1}{\rho}\frac{dp}{dL} \qquad \text{(B5)}$$

$$\frac{dp}{dL} = \frac{\gamma p}{\rho}\frac{d\rho}{dL} \quad . \qquad \text{(B6)}$$

In the above system of equations, the density ρ, the velocity u and the pressure p are all functions of the similarity variable L, which is equal to the radial location r divided by the time t. For a spherical geometry (α=3), Eqs. (B4) - (B6) reduce to those formulated by Taylor[10]. These equations can be further reduced to a set of two equations in the dependent variables u and a, the sound speed, which is a function of p and ρ. For a mixture of perfect gases, using

$$a^2 = \frac{\gamma p}{\rho} \qquad \text{(B7)}$$

and appropriately combining Eqs. (B4) - (B6) we have:

$$\frac{da^2}{dL} = -(\gamma-1)(u-L)\frac{du}{dL} \qquad \text{(B8)}$$

and

$$\frac{du}{dL} = -(\alpha-1)\frac{u}{L}\left[1 - \left(\frac{u-L}{a}\right)^2\right]^{-1} \quad . \qquad \text{(B9)}$$

The boundary conditions for obtaining the flow field between the shock wave and the piston surface are: just ahead of the piston surface

$$L_p = \frac{r_p}{t} = u_p \tag{B10}$$

and just behind the shock,

$$L_s = \frac{r_s}{t} = S_u \,, \tag{B11}$$

$$a_s^2 = \frac{\gamma p_s}{\rho_s} \,, \tag{B12}$$

and

$$u = u_s \,. \tag{B13}$$

Normal shock relations can be used to estimate u_s, ρ_s and p_s for a shock of known velocity, S_u.

Taylor solved the equivalent of Eqs. (B8) and (B9) in spherical coordinates to obtain the properties of the airwave surrounding an expanding sphere[10]. He first assumed a piston Mach number and then numerically integrated the equations from the piston surface to different locations ahead of it. He then solved the normal shock relations for various shock strengths. When he plotted these two solutions, he found that there was a location in the flow field ahead of the piston which had the same physical conditions (velocity and sound speed) as that behind a shock wave of a particular Mach number. Therefore, he could uniquely relate the flow field

ahead of a piston of given Mach number to that behind a particular shock wave. The existence of such a unique solution implies that a constant velocity piston will produce a constant velocity shock wave (in a spherical geometry). Since we find that such solutions exist in cylindrical geometries too, we can say that a constant velocity piston will produce a constant velocity shock wave in planar, cylindrical and spherical geometries provided we have a similarity solution.

We have adopted a different approach to solve Eqs. (B8) and (B9). For a shock of given Mach number, we determine the flow conditions behind it using the normal shock relations given in Appendix C. Knowing a_s and u_s, Eqs. (B8) and (B9) can be numerically integrated from L_s to the piston location L_p to give u_p and a^2_p. However we do not know L_p a priori. So we have to solve the equations until we find a L_p which is equal to u_p [See Eq. (B10)]. Therefore it is more convenient to rewrite Eqs. (B8) and (B9) in terms of a new dependent variable u/L. Then, we can solve the equations from u_s/L_s to 1.

Transforming Eqs. (B8) and (B9) to the new dependent variable ξ, where

$$\xi = \frac{u}{L} \tag{B14}$$

and defining

$$\eta = \frac{a^2}{L^2} \tag{B15}$$

and

$$z = \log_e L, \tag{B16}$$

we have

$$\frac{d\eta}{d\xi} = \frac{\eta[2\eta - 2(1-\xi)^2 - \xi(\alpha-1)(\alpha-1)(\gamma-1)(\xi-1)]}{\xi[\alpha\eta - (1-\xi)^2]} \qquad \text{(B17)}$$

and

$$\frac{dz}{d\xi} = \frac{-1}{\xi} \frac{\eta - (1-\xi)^2}{[\alpha\eta - (1-\xi)^2]} \; . \qquad \text{(B18)}$$

Eqs. (B17) and (B18) are solved along with the boundary conditions given below. Just behind the shock, that is, at

$$\xi_s = \frac{u_s}{S_u} \quad , \qquad \text{(B19)}$$

$$z = \log_e (S_u) \qquad \text{(B20)}$$

and

$$\eta = \frac{a_s^2}{S_u^2} \quad . \qquad \text{(B21)}$$

Just ahead of the piston surface,

$$\xi_p = \frac{u_p}{L_p} = 1 \quad . \qquad \text{(B22)}$$

From the solution of Eqs. (B17) and (B18), we get z_p and η_p. Using these quantities in the equations given below we calculate u_p and a_p,

$$u_p = \exp(Z_p) \tag{B23}$$

$$a_p^2 = \eta_p u_p^2 \quad . \tag{B24}$$

In addition to u_p (from Eq. (B23)) we also need the pressure at the piston surface which we can get using Eq. (B24) in the following equation,

$$p_p = p_s \left(\frac{a_p}{a_s}\right)^{\frac{2\gamma}{\gamma-1}} \quad . \tag{B25}$$

To complete the solution procedure we still need the fluid velocity, the pressure and the sound speed just behind the shock wave for (Eqs. (B19), (B21) and (B25)). Since we are restricting our attention in this paper to one dimensional flows, we can use normal shock relations to obtain these quantities. The normal shock relations, assuming that γ (the ratio of specific heats) can vary across the shock wave, have been derived in Appendix C.

Appendix C

Flow Conditions across the Shock Wave

Since we are considering only a one-dimensional flow, the flow across the shock wave along any streamline in the three geometries can be obtained from normal shock relations[15]. However, we note that it is important to use the appropriate values for γ, the ratio of specific heats, in the shocked region. Since the normal shock relations are usually obtained assuming γ constant across the shock wave, below we give a brief derivation of the normal shock relations with variable γ.

For an adiabatic, constant area, one-dimensional flow with a normal shock, the equations of continuity, momentum and energy are[15]:

$$\rho_o v_o = \rho_s v_s \tag{C1}$$

$$p_o + \rho_o v_o^2 = p_s + \rho_s v_s^2 \tag{C2}$$

$$h_o + \frac{1}{2} v_o^2 = h_s + \frac{1}{2} v_s^2 , \tag{C4}$$

where the subscript "o" refers to the conditions ahead of the shock wave and the subscript "s" refers to conditions behind the shock wave. We also need an additional constitutive relation to complete the system of equations since there are four unknowns. For a mixture of perfect gases, the caloric equation of state can be written as

$$h = f(p, \rho)$$

$$= \frac{\gamma}{\gamma - 1} \frac{p}{\rho} + h^*_{ref} \quad . \tag{C4}$$

Assuming that the gas mixture is perfect on each side of the shock wave but with different values of γ, we have:

$$h_o = \frac{\gamma_o}{\gamma_o - 1} \frac{p_o}{\rho_o} \tag{C5}$$

and

$$h_s = \frac{\gamma_s}{\gamma_s - 1} \frac{p_s}{\rho_s} \quad . \tag{C6}$$

Eliminating v_s from Eqs. (C1) and (C2), we have:

$$p_s = p_o + \rho_o v_o^2 (1 - R) \tag{C7}$$

where

$$R = \frac{\rho_o}{\rho_s} \quad . \tag{C8}$$

From Eq. (C1) we also have the fluid velocity behind the shock (in the laboratory coordinate system),

$$u_s = v_o - v_s = v_o (1 - R) \quad . \tag{C9}$$

The speed of sound behind the shock is

$$a_s = \left(\frac{\gamma_s p_s}{\rho_s}\right)^{1/2} \qquad (C10)$$

Given the initial conditions (ρ_o, p_o, v_o) ahead of the shock, we can obtain the required parameters p_s, u_s and a_s from Eqs. (C7), (C9) and (C10) if we know the parameter R.

By appropriately combining Eqs. (C1) - (C4) we have obtained the following quadratic equation for R:

$$R^2(1 + \gamma_s) - R(1 + C_1)\, 2\gamma_s + (\gamma_o C_2 + 1)(\gamma_s - 1) = 0 \qquad (C11)$$

where

$$C_1 = \frac{p_o}{\rho_o v_o^2} \quad \text{and} \quad C_2 = \frac{2C_1}{(\gamma_o - 1)} \quad . \qquad (C12)$$

From Eq. (C11), we have

$$R = \frac{\gamma_s(1 + C_1) \pm \left(\gamma_s^2 (1 + C_1)^2 - (1 + \gamma_s)(\gamma_s - 1)(\gamma_o C_2 + 1)\right)^{1/2}}{(1 + \gamma_s)} \qquad (C13)$$

The importance of using a variable γ for obtaining power-energy relations has been discussed in detail in the main text.

Effect of Temperature on the Ratio of Specific Heats

In order to use the above formulation we need to know the ratio of specific heats both ahead of the shock (γ_o) as well as that behind it (γ_s). In general, these two γ's are different because of differences in the temperature and the mixture composition. For our particular problem

the mixture composition may be assumed to be frozen across the shock wave since we are primarily interested in the mixtures up to the time when ignition occurs. In this case the specific heat at constant pressure for the mixture can be written as[16]

$$C_p = \sum_{j=1}^{m} n_j \, (C_p^o)_j \qquad \text{(C14)}$$

where n_j is in units of the Kg moles of species j per Kg of mixture and $(C_p^o)_j$ is the standard state constant pressure specific heat for species j in J/(Kg mole)(K).

For each species, the specific heat at constant pressure has been given in the form of least square coefficients in Ref. 16 as follows:

$$\frac{(C_p^o)_j}{R} = a_{1_j} + a_{2_j}T + a_{3_j}T^2 + a_{4_j}T^3 + a_{5_j}T^4 \qquad \text{(C15)}$$

where R is the universal gas constant and is equal to 8314.3 J/(Kg mole)(K). Assuming the mixture behaves like a perfect gas, we can write the ratio of specific heats, γ, as:

$$\gamma = \frac{C_p}{C_p - R} \qquad \text{(C16)}$$

or to use the data in Ref. 16 more directly,

$$\gamma = \frac{C_p/R}{C_p/R - 1} \quad . \qquad \text{(C17)}$$

Acknowledgments

The authors greatfully acknowledge suggestions, useful conversations with, and help from Jay P. Boris and T.R. Young. The authors also acknowledge the editorial assistance of Ms. F. Rosenberg. This work has been supported by the Office of Naval Research through the Naval Research Laboratory.

REFERENCES

1. Zeldovich, Y.B., Kogarko, S.M. and Simonov, N.N.: Soviet Phys.-JETP 1, 1689 (1956).

2. Litchfield, E.L., Hay, M.H. and Forshey, D.R.: Ninth Symposium (International) on Combustion, p. 282, Academic Press, 1963.

3. Freiwald, H. and Koch, H.W.: Ninth Symposium (International) on Combustion, p. 275, Academic Press, 1963.

4. Bach, G.G., Knystautas, R. and Lee, J.H.: Thirteenth Symposium (International) on Combustion, p. 1097, The Combustion Institute, 1971.

5. Lee, J.H., Knystautas, R. and Guirao, C.M.: Fifteenth Symposium (International) on Combustion, p. 53, The Combustion Institute, 1975.

6. Knystautas, R. and Lee, J.H.: Combust. Flame 27, 221 (1976).

7. Dabora, E.K.: Effect of Additives on the Lean Detonation Limit of Kerosene Sprays. UCONN0507-129-F, The University of Connecticut, 1980.

8. Dabora, E.K.: The Relation between Energy and Power for Direct Initiation of Hydrogen-Air Detonations. Presented at the Second International Workshop on the Impact of Hydrogen on Water Reactor Safety, Albuquerque, New Mexico, Oct. 1982.

9. Abouseif, G.E. and Toong, T.Y.: Combust. Flame 45, 39 (1982).

10. Taylor, G.I.: Proc. Roy. Soc. A. 186, 273 (1946).

11. Chu, B.-T.: NACA TN 3411, 1955.

12. Urtiew, P.A. and Oppenheim, A.K.: Eleventh Symposium (International) on Combustion, p. 665, The Combustion Institute, 1967.

13. Edwards, D.H., Thomas, G.O. and Williams, T.L.: Combust. Flame 43, 187 (1981).

14. Kailasanath, K. and Oran, E.S.: The Relation Between Power and Energy in the Shock Initiation of Detonations - II. Application to Hydrogen - Air Mixtures. NRL Memorandum Report (in preparation, 1983).

15. Liepmann, and Roshko: Elements of Gasdynamics, John Wiley and Sons, Inc., New York, NY, 1957.

16. Gordon, S. and McBride, B.J.: Computer - Program for Calculation of Complex Chemical Equilibrium Compositions, Rocket performance, Incident and Reflected Shocks, and Chapmann-Jouguet Detonations. NASA SP-273, 1976. N-78-17724/3.

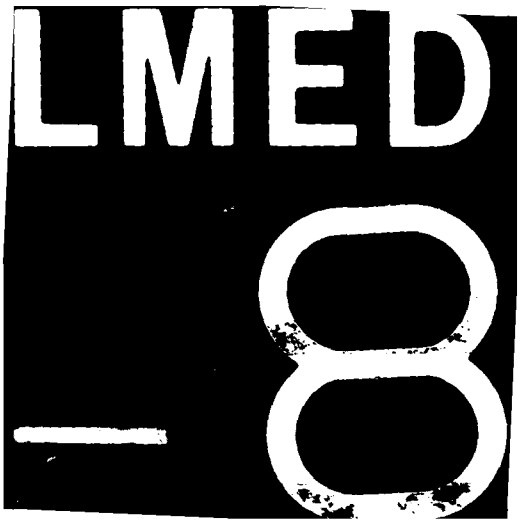
LMED
8